www.elsevier.com/locate/dsr2

Ocean acidification and calcium carbonate saturation states in the coastal zone of the West Antarctic Peninsula

Elizabeth M. Jones, Mairi Fenton, Michael P. Meredith, Nicola M. Clargo, Sharyn Ossebaar, Hugh W. Ducklow, Hugh J. Venables, Hein J.W. de Baar

PII: S0967-0645(17)30024-3
DOI: http://dx.doi.org/10.1016/j.dsr2.2017.01.007
Reference: DSRII4190

To appear in: *Deep-Sea Research Part II*

Received date: 3 February 2016
Revised date: 17 January 2017
Accepted date: 17 January 2017

Cite this article as: Elizabeth M. Jones, Mairi Fenton, Michael P. Meredith Nicola M. Clargo, Sharyn Ossebaar, Hugh W. Ducklow, Hugh J. Venables and Hein J.W. de Baar, Ocean acidification and calcium carbonate saturation states i the coastal zone of the West Antarctic Peninsula, *Deep-Sea Research Part I* http://dx.doi.org/10.1016/j.dsr2.2017.01.007

Ocean acidification and calcium carbonate saturation states in the coastal zone of the West Antarctic Peninsula

Elizabeth M. Jones[1,2]*, Mairi Fenton[3], Michael P. Meredith[3], Nicola M. Clargo[2], Sharyn Ossebaar[2], Hugh W. Ducklow[4], Hugh J. Venables[3], Hein J.W. de Baar[2,5]

[1]Centre for Energy and Environmental Sciences, University of Groningen, Nijenborgh 4, 9747 AG, Groningen, The Netherlands

[2]NIOZ Royal Netherlands Institute for Sea Research, Department of Ocean Systems, and Utrecht University, P.O. Box 59, 1790 AB Den Burg, Texel, The Netherlands

[3]British Antarctic Survey, High Cross, Madingley Road, Cambridge CB3 0ET, UK

[4]Lamont-Doherty Earth Observatory, Palisades, NY 10964, USA

[5]Ocean Ecosystems, University of Groningen, Nijenborgh 7, 9747 AG, Groningen, The Netherlands

*Corresponding author at: Centre for Energy and Environmental Sciences, University of Groningen, Nijenborgh 4, 9747 AG, Groningen, The Netherlands email: e.m.jones@rug.nl

Abstract

The polar oceans are particularly vulnerable to ocean acidification; the lowering of seawater pH and carbonate mineral saturation states due to uptake of atmospheric carbon dioxide (CO_2). High spatial variability in surface water pH and saturation states (Ω) for two biologically-important calcium carbonate minerals calcite and aragonite was observed in Ryder Bay, in the coastal sea-ice zone of the West Antarctic Peninsula. Glacial meltwater and melting sea ice stratified the water column and facilitated the development of large phytoplankton blooms and subsequent strong uptake of atmospheric CO_2 of up to 55 mmol m^{-2} day^{-1} during austral summer. Concurrent high pH (8.48) and calcium carbonate mineral supersaturation (Ωaragonite ~3.1) occurred in the meltwater-influenced surface ocean. Biologically-induced increases in calcium carbonate mineral saturation states counteracted any effects of carbonate ion dilution. Accumulation of CO_2 through remineralisation of additional organic matter from productive coastal waters lowered the pH (7.84) and caused deep-water corrosivity (Ωaragonite ~0.9) in regions impacted by Circumpolar Deep Water. Episodic mixing events enabled CO_2-rich subsurface water to become entrained into the surface and eroded seasonal stratification to lower surface water pH (8.21) and saturation states (Ωaragonite ~1.8) relative to all surface waters across Ryder Bay. Uptake of atmospheric CO_2 of 28 mmol m^{-2} day^{-1} in regions of vertical mixing may enhance the susceptibility of the surface layer to future ocean acidification in dynamic coastal environments. Spatially-resolved studies are essential to elucidate the natural variability in carbonate chemistry in order to better understand and predict carbon cycling and the response of marine organisms to future ocean acidification in the Antarctic coastal zone.

Keywords

carbonate chemistry; ocean acidification; sea ice; glacial meltwater; West Antarctic Peninsula; Ryder Bay

1. Introduction

The rapid increase of carbon dioxide (CO_2) in the atmosphere due to human activities is causing shifts in ocean chemistry, as oceanic CO_2 uptake lowers seawater pH and the concentration of carbonate ions in the process of ocean acidification (Caldeira and Wickett, 2003; Feely et al., 2004; Orr et al., 2005; Royal Society, 2005). Dissolving CO_2 in the ocean increases the partial pressure of CO_2 (pCO_2) and the concentration of dissolved inorganic carbon (C_T) in seawater (Feely et al., 2004; Takahashi et al., 2009). An immediate impact of ocean acidification on marine ecosystems is lowering of the saturation state (Ω) of calcium carbonate minerals in seawater (Feely et al., 2004; Millero, 2007; Fabry et al., 2008). Waters become corrosive to un-protected calcareous shells and skeletons when undersaturation with respect to calcium carbonate saturation states (Ω <1) occurs (Andersson et al., 2005; Royal Society, 2005; Doney et al., 2009). Biogenic carbonate minerals exist as one of two crystalline forms, aragonite or calcite, where aragonite is the less stable form and reaches undersaturation and dissolution in advance of calcite (Mucci, 1983; Orr et al., 2005). Ocean acidification as a result of anthropogenic CO_2 uptake has led to a shallowing of the aragonite saturation horizon (Ω = 1) in the water column, such that corrosive waters can flow above the depth of shelf breaks and enter coastal regions (Sabine et al., 2004; Feely et al., 2008; Bates et al., 2009). Oceanic CO_2 timeseries data show that the surface ocean concentrations of CO_2 are following the atmospheric CO_2 increase (Bates et al., 2014). The pH of the global oceans has reduced by 0.1 units over the last 200 years (Caldeira and Wickett, 2003) and is predicted to drop by a further 0.3-0.4 units by 2100 (Feely et al., 2004; Orr et al., 2005).

The polar oceans are particularly vulnerable to ocean acidification as the cold waters are naturally CO_2-rich and have a low total alkalinity (A_T) to C_T ratio that reduces the degree of carbonate mineral saturation and the buffering capacity for further CO_2 uptake (Egleston et al., 2010; Shadwick et al., 2011; Shadwick et al., 2013; Takahashi et al., 2014). Additionally, the solubility of calcium carbonate minerals increases at lower temperatures (Zeebe and Wolf-Gladrow, 2001). Climatological data from Drake Passage have revealed decreasing time-trends in surface water pH with an associated reduction in the saturation states of calcite and aragonite of -0.09 ± 0.08 and -0.06 ± 0.05, respectively, per decade (Takahashi et al., 2014). Surface waters of the Southern Ocean are predicted to experience wintertime aragonite undersaturation by 2030, driven by seasonal variations and a synergy of reduced sea-ice cover, surface water freshening and increased air-sea CO_2 exchange (Orr et al., 2005; McNeil and

Matear, 2008; Steinacher et al., 2009; Sasse et al., 2015). This has implications for pelagic and benthic calcifiers, such as Southern Ocean pteropods (Bednaršek et al., 2012), foraminifera (Moy et al., 2009) and other Antarctic molluscs (McClintock, et al., 2009) that have already shown reduced calcification and shell dissolution under acidification pressures. Furthermore, shifts in ocean chemistry influence Antarctic phytoplankton productivity, the biological carbon pump and community composition in the Southern Ocean (Neven et al., 2011; Trimborn et al., 2013). However, Antarctic sea urchins and other calcifiers have shown resilience to ocean acidification (Orr et al., 2005; Ericson et al., 2010).

The West Antarctic Peninsula (WAP) is a highly productive marine ecosystem with an effective biological carbon pump that creates important sinks for atmospheric CO_2 in the coastal sea-ice zone of the Southern Ocean (Arrigo et al., 2008b; Ducklow et al., 2007; Clarke et al., 2008). Primary production is strongly influenced by the seasonal advance and retreat of sea ice and the eastward flowing Antarctic Circumpolar Current (ACC) that impacts the western shelf of the Antarctic Peninsula. The proximity of the ACC to the WAP shelf allows warm Circumpolar Deep Water (CDW) to intrude into glacially-eroded canyons, which act as conduits to channel the CDW into the coastal zone (Martinson et al., 2008; Meredith et al., 2008; Moffat et al., 2009; Klinck and Dinniman, 2010). Mixing of CDW with overlying Antarctic Surface Water (AASW) and subsurface waters across the WAP shelf results in a modified form of CDW that occupies deep levels of the coastal areas (Klinck, 1998; Smith et al., 1999). Meltwater inputs form the fresh and less-dense AASW that overlies the permanent pycnocline and the warm, saline and CO_2-rich CDW beneath (Meredith et al., 2013). Seasonal warming and freshening stratify the upper ocean to cap a cold and saline remnant of the winter mixed layer, termed the Winter Water, at around 100 m depth (Mosby, 1934). Mixing of the AASW and Winter Water with CDW provides a supply of heat, nutrients and CO_2 to the upper ocean, which stimulates some the of highest rates of phytoplankton primary production in the whole of the Southern Ocean (Prezelin et al., 2000; Arrigo et al., 2008a; Wallace et al., 2008).

Ocean carbonate chemistry and air-sea CO_2 exchange along the WAP is strongly regulated by primary production, sea-ice dynamics, glacial meltwater inputs and the mixing of water masses (Carrillo and Karl, 1999; Carrillo et al., 2004; Wang et al., 2009; Montes-Hugo et al., 2010; Tortell et al., 2015; Hauri et al., 2015; Legge et al., 2015; Eveleth et al., 2016). The dominant freshwater source to the region is meteoric (glacial meltwater and precipitation) with a contribution from melting sea ice (Meredith et al., 2008; Meredith et al., 2010). Meltwater inputs stabilise the water column whereas reductions in winter sea-ice cover leads to deep mixing and reduced stratification the following summer (Venables and Meredith, 2014). Melting glaciers and sea ice have been found to be a source of iron that fuel phytoplankton blooms in the Antarctic (Alderkamp et al., 2012; Gerringa et al., 2012; Annett et al., 2015). Enhanced biological carbon uptake has been observed in the wake of retreating sea ice in the coastal

Antarctic (Gibson and Trull, 1999; Sweeney, 2003; Roden et al., 2013) and Southern Ocean (Bakker et al., 2008; Jones et al., 2010; Jones et al., 2015). Freshwater inputs can enhance carbonate mineral undersaturation as the concentration of carbonate ions becomes diluted, as observed in the Arctic Ocean (Yamamoto-Kawai et al., 2009; Chierici and Fransson, 2009; Bates et al., 2009; Azetsu-Scott et al., 2010; Evans et al., 2014). However, strong primary production in the coastal zone of the WAP increases carbonate mineral saturation states and compensates any dilution effects (Mattsdotter Björk et al., 2014; Hauri et al., 2015).

The timing and longevity of phytoplankton blooms and biological CO_2 drawdown is strongly influenced by seasonal sea-ice cover, which impacts light availability and water column stratification (Stammerjohn et al., 2008; Vernet et al., 2008; Venables et al., 2013). Wintertime cooling and sea-ice formation create deep mixed layers of Winter Water, during which vertical entrainment of CDW can occur (Meredith et al., 2004; Clarke et al., 2008). Sea-ice cover reduces light levels in the upper ocean and acts as a barrier to impede air-sea CO_2 exchange, enabling CO_2 enrichment in the underlying water (Delille et al., 2014). During spring and summer, retreat of the ice pack and glacial meltwater inputs promote the formation of large phytoplankton blooms through increased light levels, water column stratification and potential seeding by sea-ice algae and nutrients (Smith and Nelson, 1985; Clarke et al., 2008; Vernet et al., 2008; Meredith et al., 2013; Venables et al., 2013). The intensification of the biological carbon pump through photosynthetic carbon uptake and production and export of organic matter creates strong seasonal CO_2 sinks in coastal zones of the WAP and Antarctica (Gibson and Trull, 1999; Carillo et al., 2004; Montes-Hugo et al., 2009; Wang et al., 2009; Buesseler et al., 2010; Montes-Hugo et al., 2010; Roden et al., 2013; Legge et al., 2015).

The WAP has experienced rapid changes in atmospheric and oceanic warming over the latter part of the twentieth century (Vaughan et al., 2003; Meredith and King, 2005; Martinson et al., 2008; Martinson et al., 2012). Many of the glaciers along the WAP have rapidly retreated and there has been a reduction in sea-ice cover and shortening of the sea-ice season (Stammerjohn et al., 2012; Meredith et al., 2013; Ducklow et al., 2013; Cook et al., 2016). These changes impact upon biological production (Mitchell and Holm-Hansen, 1991; Montes-Hugo et al., 2009) and the dynamics of carbonate chemistry and atmospheric CO_2 drawdown (McNeil and Matear, 2008; Steinacher et al., 2009; Montes-Hugo et al., 2010). Ryder Bay (northern Marguerite Bay), Adelaide Island, is fringed with several marine-terminating glaciers with variable seasonality in sea-ice cover and extent. The modified CDW from the WAP shelf flows along the Marguerite Trough to supply the upper ocean with warm, nutrient-rich deep water (Martinson et al., 2008; Meredith et al., 2010). Exchange of water masses between Ryder Bay and northern Marguerite Bay occurs across a sill at 350 m depth. Warming of ACC-derived CDW and enhanced inputs of deep waters onto the WAP shelf have contributed to the degradation of glaciers and changes in sea-ice dynamics (Martinson et al., 2012; Prichard et al., 2012). The southward flowing

Antarctic Peninsula Coastal Current enters the region along the coast of Adelaide Island and generates a predominantly cyclonic circulation in Marguerite Bay (Beardsley et al., 2004; Moffat et al., 2008). Melting glaciers, sea-ice formation and melting, and mixing of the water masses influence the physical characteristics of the water column of Ryder Bay (Clarke et al., 2008; Meredith et al., 2008; Wallace et al., 2008; Meredith et al., 2010). These processes strongly regulate primary productivity and biogeochemical cycling and as such, Ryder Bay can be considered as an ideal natural laboratory to study oceanic CO_2-carbonate chemistry in a dynamic Antarctic coastal environment. This study complements the existing time series studies conducted in Ryder Bay through detailed descriptions of the spatial state of carbonate mineral saturation and pH and the controlling factors that influence ocean acidification in the coastal sea-ice zone of the WAP.

2. Methods

2.1. Seawater and ice sampling

Biogeochemical samples and physical measurements were collected in austral summer (January to March 2014) in Ryder Bay, a glacially-carved embayment (maximum depth 520 m) in northern Marguerite Bay, Adelaide Island, on the West Antarctic Peninsula (Fig. 1). This was a complement to the Rothera Time Series (RaTS) programme of the British Antarctic Survey. Long-term monitoring at this site, located about 4 km offshore from Rothera Research Station, has been carried out since 1997 (Clarke et al., 2008; Venables et al., 2013). Figure 1 shows the sampling locations used in this study: main time series site (RaTS1), secondary time series site (RaTS2), mouth of Ryder Bay (site A), along the glaciated coast (sites B, C, D), in front of Sheldon Glacier (site F), close to Horton and Hurley Glaciers (sites G,I) and proximal to Léoni Island (site J) and Lagoon Island (site K).

Vertical profiles of potential temperature and salinity were obtained using a conductivity, temperature, depth (CTD) sensor (Seabird SBE19+) attached to a line equipped with several 3.5 L Niskin bottles deployed from a rigid inflatable boat. Seawater samples for carbonate chemistry were drawn from Niskin samplers into 250 ml borosilicate glass bottles and returned to the laboratory for immediate analysis or stored for 1 week, whereby 50 μL saturated mercuric chloride solution was added. Samples for macronutrient analyses were taken from the Niskin samplers into pre-rinsed 200 ml Nalgene© plastic bottles, kept in the dark and returned to the laboratory for processing. Sea-ice and glacial-ice samples were collected between November 2014 and March 2015. Sea-ice samples were taken from fast ice in Hangar Cove, north of Ryder Bay and adjacent to Rothera Research Station. Glacial-ice samples were taken from the Sheldon Glacier (Fig. 1). Ice samples were collected into plastic, sealable bags in the field and transferred into 1 L Tedlar bags and sealed in the laboratory. The

residual air was evacuated using a Nalgene© hand pump. The samples were allowed to melt at ambient temperature (18-20°C) in the dark. Upon complete ice melt (20-24 hours), samples were transferred to 250 mL borosilicate glass bottles, poisoned with 50 μL saturated mercuric chloride solution and stored in the dark until analysis (as above).

Two sites (LMG1, LMG2) were occupied in Marguerite Bay by ARSV Laurence M. Gould on 18 January 2014. Vertical profiles of potential temperature and salinity were obtained using a CTD sensor (Seabird SBE911+) mounted onto a General Oceanics rosette equipped with 12 L Niskin bottles. The mixed layer depth (MLD) is defined as the depth where the potential density exceeds that at 2 m by 0.05 kg m^{-3}, based on definitions in Venables et al. (2013). The depth of the potential temperature minimum (θ_{min}) is taken to represent the core of the Winter Water, typically at 75-100 m (Table 1). Salinity values are reported on the practical salinity scale. Ocean Data View 4 (http://odv.awi.de) was used for data visualisation.

2.2. Analytical methods

Seawater and ice meltwater samples for total dissolved inorganic carbon (C_T) and total alkalinity (A_T) were analysed at Rothera Research Station using a VINDTA 3C (Versatile INstrument for the Determination of Total Alkalinity, Marianda) following methods prescribed in Dickson et al. (2007). Determination of C_T was made through sample acidification with 8.5% H_3PO_4 and gas extraction with coulometric analysis (Johnson et al., 1987) and A_T by automated potentiometric titration with 0.1 M hydrochloric acid (Dickson, 1981). Analyses of Certified Reference Material (CRM, batch 130) supplied by A.G. Dickson (Scripps Institute of Oceanography) every 10-20 samples were used to calibrate the measurements. The precision of the C_T and A_T measurements was 1.6 and 1.0 μmol kg^{-1}, respectively, based on the average difference between CRM in-bottle duplicate analyses (n = 47).

The Lamont-Doherty Earth Observatory (LDEO) measured surface underway pCO_2 ($pCO_{2\ ship}$) aboard ARSV Laurence M. Gould (LMG) with a precision of 0.5%, together with salinity and temperature using a shower-type water-gas equilibrator and infrared CO_2 gas analyser (see www.ldeo.columbia.edu/pi/CO2 for the operational and engineering details; Takahashi et al., 2015). A range of five standard gas mixtures spanning between 100 and 700 ppm mole fraction CO_2 certified by the Earth System Research Laboratory of the National Oceanic and Atmospheric Administration (NOAA) was used to calibrate the system every 4 hours. The mean atmospheric CO_2 mixing ratio (xCO_2) measured during 18 January 2014 (at and between sites RaTS1, LMG1, LMG2) was 393 ± 1 ppm (n = 45), consistent with the mean xCO_2 during January-March 2014 of 394 ± 3 ppm (n = 18) measured at Palmer Station, 64.77°S 64.05°W (Dlugokencky et al., 2014). Air pCO_2 was determined as a product of xCO_2 and barometric pressure, corrected for water vapour pressure (Weiss and Price, 1980), where

atmospheric pressure measured at Rothera was processed into daily means. Seawater pCO_2 was determined from xCO_2 using the solubility of CO_2 as a function of temperature and salinity (Weiss, 1974) with corrections for water vapour pressure (Weiss and Price, 1980).

For macronutrient analyses, filtered (0.2 µM) seawater and ice meltwater was collected into pre-rinsed 5 mL polyethylene vials and stored at 4°C for silicate samples and at −20°C for nitrate and phosphate samples. All analyses were carried out with a Technicon TRAACS 800 Auto-analyzer at the Royal Netherlands Institute for Sea Research, Texel. During each run a daily freshly diluted nutrient standard was measured in triplicate to monitor the performance of the analyzer. Precision for silicate, phosphate and nitrate is determined as 0.6 µmol L^{-1}, 0.016 µmol L^{-1}, 0.13 µmol L^{-1}, respectively.

2.3. CO_2-carbonate chemistry

The saturation states (Ω) of $CaCO_3$ minerals calcite and aragonite, pH in the total scale (pH_T) and pCO_2 ($pCO_{2\ AT\text{-}CT}$) were calculated from C_T and A_T, accompanied by in-situ temperature, salinity, pressure and nutrient concentrations using the CO2SYS program (Lewis and Wallace, 1998; van Heuven, 2011). The equilibrium equations of Zeebe and Wolf-Gladrow (2001) with carbonic acid dissociation constants (pK_1 and pK_2) of Mehrbach et al. (1973) as refit by Dickson and Millero (1987) were selected. These dissociation constants are appropriate for the A_T-C_T input pair in the range of temperatures and salinities in this study. Values for dissociation constants K_1 and K_2 and solubility product K_{sp} for calcite and aragonite are pressure-corrected (Mucci, 1983; van Heuven, 2011). Saturation states are a measure of the thermodynamic potential of $CaCO_3$ to precipitate or dissolve; when $\Omega < 1$ seawater becomes corrosive to calcifying organisms.

Shipboard sea surface pCO_2 values at sites RaTS1, LMG1 and LMG2 on 18 January 2014 were 161 ± 4 µatm, 158 ± 6 µatm and 172 ± 13 µatm, respectively, and were used for consistency checks between measured ($pCO_{2\ ship}$) and calculated ($pCO_{2\ AT\text{-}CT}$) seawater values (Table 1). The ΔpCO_2 is the difference between $pCO_{2\ AT\text{-}CT}$ in surface seawater and the daily mean air pCO_2 value. Fluxes of CO_2 (Equ. 1) were calculated from ΔpCO_2, solubility of CO_2 (K_0) and the gas transfer coefficient (k), which is a function of wind speed (Wanninkhof et al., 2013).

$$CO_2 \text{flux} = k \cdot K_0 \cdot \Delta pCO_2 \quad (1)$$

Fluxes of CO_2 were calculated using wind speed data measured at Rothera, taken as a mean over the growing season until the time of sampling (Δt; Table 1) and corrected to 10 m above sea level (Hartman and Hammond, 1985). Negative values of ΔpCO_2 and CO_2 flux indicate CO_2 undersaturation with respect to the atmosphere and uptake of atmospheric CO_2.

3. Results

3.1. Summer sea surface of Ryder Bay

The salinity along the glaciated coastline was low (S <32.8) due to meltwater influence (Fig. 2a and b). Sea surface temperature varied from −0.6 °C to 1.7 °C with warmer waters typically located closer to the coast (Fig. 2c). Low concentrations of C_T (<2000 μmolkg^{-1}) were found in this region (Fig. 2d). Surface water A_T followed a similar distribution to salinity as higher values (>2250 μmolkg^{-1}) were found in saltier water at the mouth of Ryder Bay (site A) and close to island shelves (sites J and K) (Fig. 2e). Near-depleted nitrate concentrations indicated high biological uptake in the meltwater-influenced sites (Fig. 2f). Surface waters across Ryder Bay were undersaturated ($pCO_{2\ AT\text{-}CT}$ of 119-252 μatm; Fig. 2g) with respect to atmospheric CO_2 and the whole region was a strong sink for atmospheric CO_2 (Table 1). Total scale pH (pH_T) ranged from 8.21 to 8.48 (Fig. 2h). The saturation states of aragonite and calcite had large spatial variability, ranging from 1.8 and 3.1 (Fig. 2i) and 2.9 to 5.0 (not shown), respectively.

Lowest concentrations of C_T (1911 μmolkg^{-1}), A_T (2211 μmolkg^{-1}) and strong pCO_2 undersaturation (119 μatm) were observed by melting sea ice (site D), marked by the lowest salinity (~32.1) relative to the rest of Ryder Bay. Concurrent aragonite supersaturation (Ω >2.5) occurred in this area and along the glaciated coastline. Central Ryder Bay (sites C and G) and shelf waters of Léoni and Lagoon Islands (sites J and K) were characterised by higher salinity (S >32.8) and high C_T (2055-2085 μmol kg^{-1}). The lowest pH_T (8.21) and the lowest aragonite saturation levels (1.8) near Lagoon Island (site K). The coldest water of −0.6 °C was observed in front of Sheldon Glacier (site F) with higher A_T, C_T and lower saturation states compared to other coastal sites.

3.2. Deep waters of Ryder Bay

Waters occupying the deepest levels across Ryder Bay (Fig. 3a) had higher salinity and lower temperatures (not shown) with much less variability compared to the surface layer. Exceptions were the waters overlying the shallow island shelf (site K) and in front of Sheldon Glacier (site F), where the lowest values of C_T (2166-2172 μmolkg^{-1}) and A_T (2285-2292 μmol kg^{-1}) were found. Both sites exhibited the highest deep water pH_T and aragonite saturation states (Fig. 3b-c). In contrast, the highest values of C_T (>2240 μmolkg^{-1}) and A_T (>2310 μmolkg^{-1}) occurred in deep waters of the coastal zone and in central Ryder Bay. Concurrent high nitrate concentrations (>34.2 μmolkg^{-1}) indicated remineralisation of organic matter at these locations. All deep waters had low pH_T (7.84-7.87) and were undersaturated with respect to aragonite (Ω ~0.9-1.0) across Ryder Bay.

3.3. Water mass and meltwater carbonate chemistry

Distinct water masses could be identified from salinity and potential temperature characteristics in Ryder Bay (Fig. 4a). Warm and fresh Antarctic Surface Water (AASW) occupied the summer mixed layer with high and variable aragonite saturation states (2.5 ± 0.5). The Winter Water layer was identified by a distinct potential temperature minimum and steep, decreasing gradients in aragonite saturation. The deepest levels (>200 m) of Ryder Bay and Marguerite Bay were filled with modified CDW, which was distinguished within a given salinity range ($34.6 \leq S \leq 34.7$) as measured on the shelf of the WAP from upper CDW of the ACC offshore (Smith et al., 1999). Modified CDW was found intruding the shelves of the WAP with C_T and A_T values of 2253 μmol kg^{-1} and 2350 μmol kg^{-1}, respectively (Hauri et al., 2015). The CDW identified in Marguerite Bay had potential temperature and salinity values of 1.23 ± 0.04 °C and 34.64 ± 0.01, respectively. In comparison, the CDW in Ryder Bay was cooler (1.14 ± 0.08 °C) and fresher (34.60 ± 0.03). Relative to ACC-derived CDW, the CDW in Marguerite Bay had higher concentrations of C_T (2276 ± 1 μmol kg^{-1}), whereas A_T values (2348 ± 1 μmol kg^{-1}) were similar. The CDW identified in Ryder Bay had higher C_T concentrations (2279 ± 3 μmol kg^{-1}) whereas A_T values (2348 ± 4 μmol kg^{-1}) were conserved. The shift in water mass properties is indicative of entrainment of thermocline water into the CDW (Venables et al., this issue) and organic matter remineralisation. The modified CDW across Ryder Bay was undersaturated with respect to aragonite.

The distribution of A_T and C_T relative to salinity revealed high meltwater-induced variability (Fig. 4b). Meltwater carbonate chemistry was determined for glacial ice (S = 0, C_T = 16 ± 5 μmolkg^{-1}, A_T = 100 ± 5 μmolkg^{-1}) and sea ice (S = 7, C_T = 277 ± 150 μmolkg^{-1}, A_T = 328 ± 150 μmolkg^{-1}) as a freshwater end member, similar to ~300 μmolkg^{-1} previously reported for melting sea ice (Anderson and Jones, 1985; Bates et al., 2009; Yamamoto-Kawai et al., 2009). The modified CDW end member is defined as above. Values of A_T closely followed the salinity-dilution lines with positive deviations of about 20 μmolkg^{-1} at lower salinities. This pattern indicates an excess of alkalinity in the meltwater-influenced surface waters. The salinity and C_T correlation showed strong negative C_T deviations from the theoretical mixing lines. This divergence suggests that elevated biological production removes substantial C_T between 50-200 μmolkg^{-1} in meltwater-influenced surface waters, thereby increasing aragonite saturation states.

Vertical distributions of A_T across the upper and lower sections of Ryder Bay (Fig. 5a) generally followed the trends in salinity with low values in the upper waters that increased with increasing depth (Fig. 5b-c). Concentrations of C_T increased with depth and had steep vertical gradients to the highest values in the deepest parts of the bay (200-500 m) with CDW influence (Fig. 5d and e). The lowest C_T and A_T in the upper 25 m occurred in the productive meltwater layer, which corresponded to high aragonite supersaturation (Fig. 5f and g). Weak vertical gradients of C_T near Sheldon Glacier (site F) and over the

shelf of Lagoon Island (site K) were accompanied by a deepening of the aragonite saturation horizon. From east to west across the lower part of Ryder Bay, the shoaling aragonite saturation horizon impacted the Winter Water layer with strong undersaturation at the glaciated coast (site I).

4. Discussion

4.1. Biologically-induced sea surface carbonate supersaturation and deep water acidification

Biological processes in meltwater-impacted areas had a large control on surface water calcium carbonate saturation states and pH_T across Ryder Bay. Since the saturation state for calcite is about 50% higher than that for aragonite and shows the same distribution and trend, for example in relation to pH_T (Fig. 6a), the discussions that follow will focus only on aragonite saturation states and pH_T. Aragonite supersaturation (Ω >2.0) was concurrent with surface water salinity in the range 32.1-33.1 where biological carbon uptake reduced surface water C_T to less than 1950 $\mu molkg^{-1}$ and counteracted any meltwater-induced suppression of saturation states. This theory is supported by the strong anti-correlation between saturation states with salinity where high aragonite saturation was found in the meltwater-influenced surface waters (Fig. 6b). These values fall into the range of aragonite saturation (Ω = 1.7-3.5) found in summer surface waters at other coastal sites in the Ross Sea (Sweeney, 2003) and Prydz Bay, East Antarctica (Gibson and Trull, 1999; McNeil et al., 2011) and in Southern Ocean waters close to the Antarctic Peninsula (Tynan et al., 2016).

Meltwater-stratification, high light levels and macro- and micro-nutrient supplies are essential for sustaining the large phytoplankton blooms that are characteristic of this region (Venables et al., 2013; Annett et al., 2015; Henley et al., this issue). High primary productivity and intense photosynthetic reductions in CO_2 and C_T increased summertime carbonate mineral saturation states in Ryder Bay. The hypothetical mixing relationships of glacial ice and sea ice with modified CDW indicate that biological uptake of up to 200 µmol C_T kg^{-1} was accompanied by aragonite supersaturation in surface waters. Nitrate concentrations at or close to depletion (<0.2 $\mu molkg^{-1}$) with associated low C_T of 1911-1955 $\mu molkg^{-1}$ in the surface layer showed the close coupling of nitrate and carbon cycling (Fig. 6c). Nitrate concentrations may reach transient periods of exhaustion due to phytoplankton growth but are regenerated and re-supplied in the upper water column during the summer (Henley et al., this issue). These findings support the hypothesis that biological C_T uptake was a driving force for high aragonite saturation states in the AASW. Previous studies along the WAP have also linked spatial variability in carbonate saturation states to biological productivity and meltwater inputs (Hauri et al., 2015).

Surface waters of Ryder Bay were strongly undersaturated with respect to atmospheric CO_2 (ΔpCO_2 up to −256 µatm) to create areas of substantial CO_2 uptake of up to 55.4 mmol m^{-2} day^{-1} during

austral summer. It is predicted that such strong atmospheric CO_2 uptake persists in Ryder Bay during the summer (January and February) as consistently low sea surface CO_2 coupled to high chlorophyll-a concentrations in shallow mixed layers (< 10 m) is known to occur throughout these months on an annual basis (Legge et al., 2015; Legge et al., this issue). This study found a stronger degree of CO_2 undersaturation with respect to atmospheric values compared to data from three summer seasons presented in Legge et al. (2015) and higher carbonate saturation states than those reported by Legge et al. (this issue) for January-February 2014 at 15 m depth at RaTS1. These features can be attributed to the finer-scale vertical sampling (2, 5, 15 m) in the surface layer in this study, which resolved the biological production signal in very shallow meltwater layers. Both studies confirm that favourable conditions (high light levels, nutrient supply) drive carbonate mineral supersaturation and create strong sinks for atmospheric CO_2 in Ryder Bay.

Steep vertical gradients in C_T were found from productive surface waters to the deep parts (200-500 m) of Ryder Bay that were impacted by CDW, for example C_T increased with depth by up to 2 $\mu molkg^{-1}m^{-1}$ between the AASW and CDW layers in the productive coastal zone. Biologically-driven aragonite supersaturation in high-pH_T (>8.47) surface water swiftly changed with depth to reach intense aragonite undersaturation with minimum values of pH_T of 7.84 at and below the Winter Water layer. Whilst recycling and advective losses of organic carbon in the upper water column are important components of biogeochemical fluxes in the WAP, export of at least 10% of the net primary production provides a supply of organic carbon to subsurface waters and sustains rich benthic communities (Buesseler et al., 2010; Weston et al., 2013; Constable et al., 2014; Stukel et al., 2015). The sinking particulate organic carbon in highly productive coastal waters and subsequent remineralization likely contributed to high concentrations of C_T (>2280 $\mu molkg^{-1}$) found in the CDW. Remineralisation through oxidation recycles organic material back into inorganic forms C_T and nitrate and enriches deep water concentrations with associated suppression of calcium carbonate saturation states. The proposed mechanism is supported by negative correlations of aragonite saturation states with nitrate and C_T concentrations (Fig. 6c-d).

An intensification of the biological carbon pump in the productive coastal zone generated carbonate mineral supersaturation in surface waters and undersaturation in subsurface waters, through remineralisation of exported organic material. This process was likely to further increase C_T in the CDW as it flowed inland to drive pH_T and saturation states to their minimum values in Ryder Bay. The shoaling of the aragonite saturation horizon in the coastal zone presents acidification conditions the marine communities of Ryder Bay. Antarctic benthic organisms have shown vulnerability to ocean acidification pressures that is likely influenced by local environmental conditions (Ahn, 1993; McClintock, et al., 2009; Morley et al., 2009; Cummings et al., 2011). However, contemporary distributions and natural spatio-temporal variations in carbonate mineral saturation levels suggest that pelagic-benthic organisms of the WAP and Southern Ocean may exhibit a degree of resilience to further ocean acidification (McNeil et al.,

2011). Future studies should investigate synergistic effects and analyse a range of biological variables to attain a more comprehensive view of the likely ecological impacts of Antarctic environmental change.

4.2. Impact of ice melt on carbonate mineral saturation states

Glacial meltwater is the dominant freshwater source to Ryder Bay (Meredith et al., 2008) and, combined with seasonal sea-ice melt, exerts an important influence on carbonate saturation states and pH_T. Glacial and sea'ice meltwaters were found to exhibit very low C_T-A_T signatures, which have the chemical potential to suppress carbonate mineral saturation states through dilution of carbonate ion concentrations, as found in the Arctic Ocean (Chierici and Fransson, 2009; Yamamoto-Kawai et al., 2009; Evans et al., 2014). However, this was not evident in Ryder Bay as the highest aragonite saturation states (Ω >3.0) were concurrent with the freshest (S of 32.1-32.8) surface water. Phytoplankton production probably counteracted any meltwater dilution effects as photosynthetic CO_2 uptake reduced surface water C_T, thereby decreasing the ratio of C_T to A_T and increasing the state of carbonate saturation (Bates et al., 2009). This is consistent with other observations in coastal Antarctic waters (Shadwick et al., 2013; Mattsdotter Björk et al., 2014; Hauri et al., 2015).

Surface A_T is primarily governed by meltwater inputs with contributions from carbonate mineral precipitation and dissolution and mixing into A_T-rich deep water. As phytoplankton utilise nitrate as the nitrogen source for primary production, A_T is affected through the principle of electroneutrality; uptake of nitrate (NO_3^-) removes hydrogen ions (H^+) thereby increasing A_T (Brewer and Goldman, 1976; Wolf-Gladrow et al., 2007). The concentration of nitrate in surface waters varied between 0.1-14.4 $\mu molkg^{-1}$ due to biological utilization versus re-supply from recycling in the surface layers and mixing with nitrate-rich subsurface waters (Henley et al., this issue). To compensate for the effects of nitrate changes on A_T values, potential alkalinity (A_T*; the sum of A_T and nitrate) is considered and thus resulting variability can be attributed to carbonate processes and mixing. Surface water potential alkalinity and salinity has a positive relationship (A_T* = 69.S + 2; r^2 = 0.97) and data fall between the glacial ice, sea ice and CDW mixing lines (Fig. 7). The positive deviations of A_T up to 20 $\mu molkg^{-1}$ relative to the hypothetical meltwater-seawater mixing trends revealed excess A_T in meltwater-impacted surface waters. We hypothesise that these changes may result from the dissolution of the carbonate mineral ikaite ($CaCO_3.6H_2O$), which forms in sea ice during winter (Dieckmann et al., 2008; Fransson et al., 2011; Rysgaard et al., 2012). Upon sea-ice melt, ikaite crystals dissolve to release carbonate ions (increasing alkalinity) and reduce pCO_2 in the surrounding seawater to drawdown atmospheric CO_2; the sea-ice CO_2 pump (Papadimitriou et al., 2004; Delille et al., 2007; Rysgaard et al., 2007; Geilfus et al., 2012). In addition, sea-ice meltwater may exhibit A_T-C_T deficits from residual brines where ikaite precipitation has taken place, which would also reduce sea surface pCO_2 in the meltwater layer (Jones et al., 2010).

Currents, such as the Antarctic Peninsula Coastal Current (Beardsley et al., 2004; Moffat et al., 2008), winds and tides transport sea ice into and out of Ryder Bay (Clarke et al., 2008; Meredith et al., 2008; Wallace et al., 2008; Meredith et al., 2010). As such, sea ice that formed elsewhere in the WAP may contribute additional biogeochemical characteristics upon melting in Ryder Bay. Therefore, dissolution of ikaite crystals from melting sea ice likely contributes to CO_2 drawdown during seasonal sea-ice melt in Ryder Bay, as suggested by Legge et al. (this issue).

The potential alkalinity-salinity relationship agrees with those in the Antarctic region (60-70 °S) of the Atlantic Ocean (A_T* = 58.S + 368) and in the circumpolar Southern Ocean (south of 60°S) region (A_T* = 74.S − 192) from climatological data distributions (Takahashi et al., 2014). The sign and magnitude of the slope and intercept for the Ryder Bay data fit between the two groups of climatological data and show low alkalinity typical of Antarctic waters (Egleston et al., 2010) and the influence of mixing with upwelled deep waters of higher alkalinity and salinity as typical for Antarctic shelf and coastal regions. The Ryder Bay data have a comparatively narrow range of potential alkalinity (2210-2275 μmolkg^{-1}) at lower salinities (32.1-33.1), which is attributed to glacial and sea-ice meltwater influences in the WAP coastal zone. Time series sampling with finer temporal resolution at the ice-ocean interface and within meltwater plumes would help to better understand the carbonate chemistry of meltwaters and improve climatological estimates of carbonate chemistry distributions and carbon cycling in the under-sampled Antarctic coastal zone.

4.3. Deep mixing drives weak carbonate saturation gradients

Episodic wind-driven mixing and turbulent water column conditions destabilised any stratification and eroded summer surface biological signals. Weak vertical gradients in C_T resulted from the downward mixing of productive surface waters, which allowed exchange with carbon-rich, low pH_T Winter Water and modified CDW. For example, the mixed water column overlying the shelf of Lagoon Island had a shallow gradient with an increase of 85 μmol C_T kg^{-1} between AASW and the Winter Water layer, compared to rapid C_T increases with depth, up to four times greater (332 μmolkg^{-1}) for the same depth range, along the meltwater-stratified coast. The effect of phytoplankton production over the island shelves was strongly compensated, based on relatively high residual nitrate concentrations of 14.4 μmol kg^{-1} at the sea surface and C_T values of 2085 μmol kg^{-1}, and as such mixing processes re-supplied the upper ocean with carbon and nitrate.

Coldest surface waters (–0.6 °C) near Sheldon Glacier were relatively salty (S = 32.9) compared to other coastal sites, which indicated strong vertical mixing into saline subsurface waters despite close proximity to the glacier face and meltwater inputs. Reduced nitrate (4.4-6.1 μmol kg^{-1}) and C_T (~2031 μmol kg^{-1}) showed evidence of summertime biological production with concomitant high

aragonite saturation states of 2.3 in the surface layer. These features likely resulted from episodic wind-driven mixing that recently impacted the otherwise productive water column and as such the depth of the aragonite saturation horizon deepened from its location at around 75 m across Ryder Bay. The effects of mixing and vertical water mass exchange reduced aragonite saturation states throughout the water column relative to values across Ryder Bay at Sheldon Glacier and Lagoon Island, for example ranging from 1.83 to 1.36 between AASW and the Winter Water near Lagoon Island. These waters would be particularly sensitive to future ocean acidification as summertime sea surface pCO_2 undersaturation enabled further atmospheric CO_2 uptake of 27.9 mmol m^{-2} day^{-1}, which could drive carbonate mineral undersaturation and create areas of surface water corrosivity.

4.4. A wider regional context

Key variables of CO_2-carbonate chemistry in an ocean acidification context are pH, carbonate mineral saturation states and air-sea CO_2 fluxes. Values of these variables measured in central Ryder Bay (RaTS1) were similar compared to the mean value from all other Ryder Bay sites for the air-sea CO_2 flux of −48.6 and −43.2 mmol m^{-2} day^{-1} and aragonite saturation state in AASW of 2.6 and 2.5, respectively. Winter Water aragonite saturation states at RaTS1 and the Ruder Bay mean value were both 1.1 (Table 1). Whilst large spatial variability existed during the summer, the carbonate chemistry distributions at RaTS1 can be considered as broadly representative of those of Ryder Bay. The values were put into a wider regional context by comparison to CO_2-carbonate chemistry data from Marguerite Bay. To remove temporal variability, sampling at RaTS1 and in Marguerite Bay was carried out on the same day. Shipboard measurements of sea surface pCO_2 varied between 135 µatm and 199 µatm to show that the whole region was highly undersaturated with respect to atmospheric CO_2 (Fig. 8). Variability in the degree of CO_2 undersaturation likely resulted from the balance of the dominant controls on surface water carbonate chemistry distributions in the sea-ice coastal zone, i.e., biological CO_2 drawdown versus vertical mixing with CO_2-rich subsurface waters (section 4.1 and 4.3).

Shipboard pCO_2 ($pCO_{2\ ship}$) measurements (averaged over a 30-minute period during the time of surface water C_T and A_T sampling) provide a consistency check for those calculated from C_T and A_T, $pCO_{2\ AT\text{-}CT}$, as described in section 2.3. Sea surface $pCO_{2\ AT\text{-}CT}$ at RaTS1 and in southern Marguerite Bay (LMG1) was 155 and 157 µatm, respectively, which was very close to $pCO_{2\ ship}$ of 161 ± 4 µatm (RaTS1) and 158 ± 6 µatm (LMG1). Northern Marguerite Bay (LMG2) had higher $pCO_{2\ AT\text{-}CT}$ of 187 µatm, which showed a larger offset compared to 172 ± 13 µatm as measured onboard. From the available data, $pCO_{2\ AT\text{-}CT}$ largely replicated the measured values and showed that the calculation approach for the carbonate chemistry variables is sufficiently robust within the given analytical precision. Larger offsets between measured and calculated pCO_2 (~15 µatm) as shown in northern Marguerite Bay are likely due to the

high spatial variability in surface water pCO_2 and the difference in sampling time between the automated sea surface pCO_2 system (taking seawater measurements every 3 minutes) and the closing of a surface water Niskin bottle (one snap-shot time) in moving ocean waters.

Values of the air-sea CO_2 flux (−41.7 and −44.9 mmol m^{-2} day^{-1}) and aragonite saturation states in modified CDW (1.0) in Marguerite Bay were very close when compared to those values of −44.9 mmol m^{-2} day^{-1} and 0.9 determined at RaTS1. The similarity of physical properties (Venables and Meredith, 2014) and vertical distributions of C_T-A_T (Fig. 9) between Ryder Bay and Marguerite Bay suggest that the principle processes influencing the carbonate chemistry are consistent between the two bays. The increase in absolute values of C_T between the CDW present in Ryder Bay relative to that in Marguerite Bay is likely due to modification of the water mass that includes a signal of export and remineralisation of organic carbon in the productive coastal waters. The processes impacting carbonate chemistry in Ryder Bay and Marguerite Bay are likely to also likely to occur in northern parts of the coastal sea-ice zone of the WAP, as currents such as the southward flowing Antarctic Peninsula Coastal Current advect water masses into the study area and transfer biogeochemical properties into Ryder Bay (Klinck et al., 2004; Wallace et al., 2008). Therefore, observations in Ryder Bay are likely to incorporate biogeochemical signatures from waters farther north as well as from Marguerite Bay. Spatio-temporal studies are, therefore, essential to elucidate the controls on carbon cycling in seasonally and regionally dynamic environments and to better understand ocean acidification impacts on marine ecosystems in the climatically-vulnerable Antarctic coastal waters.

5. Conclusion

High spatial variability in summertime surface water pH and carbonate mineral saturation states was observed in Ryder Bay in the coastal sea-ice zone of the West Antarctic Peninsula. Primary productivity had the largest impact on calcium carbonate mineral saturation states, generating supersaturation with respect to biogenic minerals calcite and aragonite of up to 3.1 and 5.0, respectively. Glacial meltwater and melting sea ice stratified the water column and facilitated the development of large phytoplankton blooms that resulted in high pH (8.48) and calcium carbonate supersaturation (Ω >3). The sea surface of Ryder Bay was strongly undersaturated with respect to atmospheric CO_2 as biological carbon uptake reduced seawater $pCO_{2\ AT\text{-}CT}$ to 119-252 µatm and created intense CO_2 sinks (55 mmol m^{-2} day^{-1}) in meltwater-impacted areas during austral summer. Effects of transient sea-ice melt were superimposed onto the glacial melt signal, where any carbonate ion dilution was completely compensated by biologically-driven carbon uptake and increases in carbonate mineral saturation states. The presence of excess alkalinity in sea-ice meltwater indicated that dissolution of sea ice-derived carbonates likely had minor contributions to atmospheric CO_2 drawdown during the seasonal thaw. A strong biological carbon

pump in the coastal sea-ice zone created (i) surface water calcium carbonate supersaturation and (ii) deep-water corrosivity, as additional organic debris produced in productive waters are settled to depth and remineralised, thus adding CO_2 to naturally carbon-rich Circumpolar Deep Water in the deepest levels of Ryder Bay. Deep mixing enabled entrainment of CO_2-rich waters into the surface, which supressed surface water aragonite saturation states (Ω ~1.8) and induced low vertical gradients in pH. Episodic mixing events may enhance the vulnerability of the surface layer to ocean acidification upon further uptake of anthropogenic CO_2 during the summer. Variations in calcium carbonate mineral saturation states and air-sea CO_2 fluxes across Ryder Bay can be considered as largely representative of Marguerite Bay, with relevance to the wider West Antarctic Peninsula coastal zone. The findings here highlight the importance of higher resolution sampling for the accurate assessment of carbon cycling in dynamic environments that are influenced by meltwater inputs, high productivity and mixing of water masses. These processes generated high spatial variability in oceanic carbonate chemistry, which impacted the drawdown of atmospheric CO_2 and functioning of the biological carbon pump. As such, the productive coastal sea-ice zones of Antarctica are key regions to study the response of marine ecosystems to impacts of ocean acidification.

Acknowledgements

The authors gratefully acknowledge BAS, Royal NIOZ and NWO for the opportunity to conduct fieldwork at the Dirck Gerritsz and Bonner laboratories at Rothera. Particular thanks to J. Bown, P. Rozema, S. Henley, S. Heiser for assistance in the laboratory, boating and sample collection. Support was gratefully received from S. Ober, for CTD maintenance and data calibration, and P. Laan for technical and logistical issues. Extended thanks to the scientific party, Captain, officers and crew onboard ARSV Lawrence M. Gould for the support and opportunity to sample in Marguerite Bay. Meteorological data were obtained from www.antarctica.ac.uk/met/metlog/. Atmospheric CO_2 data were obtained from NOAA at ftp://aftp.cmdl.noaa.gov/data/trace_gases/co2/flask/surface/co2_psa_surface-flask_1_ccgg_event.txt. This work is part of postdoctoral research (E. Jones) at the University of Groningen under the research programme 866.13.006, which is (partly) financed by the Netherlands Polar Programme at NWO. RaTS is a component of the Polar Oceans research programme at BAS, funded by NERC. The LMG-based sampling was supported by US NSF-ANT 1440435 (Palmer LTER) to H. Ducklow. Underway pCO_2 acquisition was supported by the Ship of Opportunity Observation Program (SOOP) and a grant (NA10OAR4320143) from the United States NOAA. We gratefully acknowledge the helpful comments of two anonymous reviewers that have considerably improved the quality of the manuscript. This work is dedicated to Dutch polar explorer Philip de Roo.

References

Ahn, I.Y., 1993. Enhanced particle flux through the biodeposition by the Antarctic suspension-feeding bivalve Laternula elliptica in Marian Cove, King George Island. J. Exp. Mar. Biol. Ecol. 171, 75-90.

Alderkamp, A-C., Mills, M.M., van Dijken, G.I., Laan, P., Thuroczy, C-E., Gerringa, L.J.A., de Baar, H.J.W., Payne, C.D., Visser, R.J.W., Buma, A.G.J., Arrigo, K.R., 2012. Iron from melting glaciers fuels the phytoplankton blooms in Amundsen Sea (Southern Ocean): Phytoplankton characteristics and productivity. Deep-Sea Res. II 71-76, 16-31.

Anderson, L.G., Jones, E.P., 1985. Measurements of total alkalinity, calcium and sulfate in natural sea ice, J. Geophys. Res. 90, 9194-9196, doi:10.1029/JC090iC05p09194.

Andersson, A.J., Mackenzie, F.T., Lerman, A., 2005. Coastal ocean and carbonate systems in the high CO_2 world of the Anthropocene. Am. J. Sci. 305, 875-918, doi:10.2475/ajs.305.9.875.

Annett, A., Skiba, M., Henley, S.F., Venables, H.J., Meredith, M.P., Statham, P.J., Ganeshram, R.S., 2015. Comparative roles of upwelling and glacial iron sources to Ryder Bay, coastal western Antarctic Peninsula. Mar. Chem. 176, 21-33.

Arrigo, K.R., van Dijken, G.L., Bushinsky, S., 2008a. Primary production in the Southern Ocean, 1997-2006. J. Geophys. Res.-Ocean. 113 (C8). http://dx.doi.org/10.1029/2007jc004551.

Arrigo, K.R., van Dijken, G., Long, M., 2008b. Coastal Southern Ocean: a strong anthropogenic CO_2 sink. Geophys. Res. Lett. 35 (21), L21602. http://dx.doi.org/10.1029/2008gl035624.

Azetsu-Scott, K., A. Clarke, K. Falkner, J. Hamilton, E. P. Jones, C. Lee, B. Petrie, S. Prinsenberg, M. Starr, Yeats, P., 2010. Calcium Carbonate Saturation States in the waters of the Canadian Arctic Archipelago and the Labrador Sea. J. Geophys. Res. 115, 375 C11021. doi:10.1029/2009JC005917.

Bakker, D.C.E., Hoppema, M., Schroder, M., Geibert, W., de Baar, H.J.W., 2008. A rapid transition from ice covered CO_2 rich waters to a biologically mediated CO_2 sink in the eastern Weddell Gyre. Biogeosciences 5, 1373-1386.

Bates, N.R., Mathis, J.T., Cooper, L.W., 2009. Ocean acidification and biologically induced seasonality of carbonate mineral saturation states in the western Arctic Ocean. J. Geophys. Res. 114, C11007. doi:10.1029/2008JC004862.

Bates, N.R., Astor, Y.M., Church, M.J., Currie, K., Dore, J.E., González-Dávila, M., Lorenzoni, L., Muller-Karger, F., Olafsson, J., Santana-Casiano, J.M., 2014. A time-series view of changing ocean chemistry due to ocean uptake of anthropogenic CO_2 and ocean acidification. Oceanography 27, 126–141. http://dx.doi.org/10.5670/oceanog.2014.16.

Bednaršek, N., Tarling, G.A., Bakker, D.C.E., Fielding, S., Jones, E.M., Venables, H.J., Ward, P., Kuzirian, A., Lézé, B., Feely, R.A., Murphy, E.J., 2012. Extensive dissolution of live pteropods in the Southern Ocean. Nature Geo. 5, 881-885. doi:10.1038/ngeo1635.

Beardsley, R.C., Limeburner, R., Owens, W.B., 2004. Drifter measurements of surface currents near Marguerite Bay on the western Antarctic Peninsula shelf during austral summer and fall, 2001 and 2002. Deep-Sea Res. II 51 (17-19), 1947-1964. http://dx.doi.org/10.1016/j.dsr.2004.07.031.

Brewer, P.G., Goldman, J.C., 1976. Alkalinity changes generated by phytoplankton growth. Limnol. Ocean. 21, 108-117.doi:10.4319/lo.1976.21.1.0108.

Buesseler, K.O., McDonnell, A.M.P., Schofield, O.M.E., Steinberg, D.K., Ducklow, H.W., 2010. High particle export over the continental shelf of the west Antarctic Peninsula. Geophys Res. Lett. 37. http://dx.doi.org/10.1029/2010gl045448.

Caldeira, K., and Wickett, M.E., 2003. Ocean model predictions of chemistry changes from carbon dioxide emissions to the atmosphere and ocean. J. Geophys. Res. 110, C09S04, doi:10.1029/2004JC002671.

Carrillo, C. J. and Karl, D. M., 1999. Dissolved inorganic carbon pool dynamics in northern Gerlache Strait, Antarctica, J. Geophys. Res. 104, 15873. doi:10.1029/1999JC900110.

Carrillo, C. J., Smith, R. C., Karl, D. M., 2004. Processes regulating oxygen and carbon dioxide in surface waters west of the Antarctic Peninsula. Mar. Chem. 84, 161-179. doi:10.1016/j.marchem.2003.07.004.

Chierici, M., Fransson, A., 2009. Calcium carbonate saturation in the surface water of the Arctic Ocean: undersaturation in freshwater influenced shelves. Biogeosciences 6, 2421-2432. doi:10.5194/bg-6-2421-2009.

Clarke, A., Meredith, M.P., Wallace, M.I., Brandon, M.A., Thomas, D.N., 2008. Seasonal and interannual variability in temperature, chlorophyll and macronutrients in northern Marguerite Bay, Antarctica. Deep-Sea Res. II 55, 1988-2006. doi:10.1016/j.dsr2.2008.04.035.

Constable, A.J., Melbourne-Thomas, J., Corney, S.P., Arrigo, K.R., Barbraud, C., Barnes, D.K.A., Bindoff, N.L., Boyd, P.W., Brandt, A., Costa, D.P., Davidson, A.T., Ducklow, H.W., Emmerson, L., Fukuchi, M., Gutt, J., Hindell, M.A., Hofmann, E.E., Hosie, G.W., Iida, T., Jacob, S., Johnston, N.M., Kawaguchi, S., Kokubun, N., Koubbi, P., Lea, M.-A., Makhado, A., Massom, R.A., Meiners, K., Meredith, M.P., Murphy, E.J., Nicol, S., Reid, K., Richerson, K., Riddle, M.J., Rintoul, S.R., Smith, W.O., Southwell, C., Stark, J.S., Sumner, M., Swadling, K.M., Takahashi, K.T., Trathan, P.N., Welsford, D.C., Weimerskirch, H., Westwood, K.J., Wienecke, B.C., Wolf-Gladrow, D., Wright, S.W., Xavier, J.C., Ziegler, P., 2014. Climate change and Southern Ocean ecosystems I: How changes in physical habitats directly affect marine biota. Glob. Change Biol. 20, 3004-3025. doi:10.1111/gcb.12623.

Cook, A.J., Holland, P.R., Meredith, M.P., Murray, T., Luckman, A., Vaughan, D.G., 2016. Ocean forcing of glacier retreat in the western Antarctic Peninsula. Science 353 (6296), 283-286. http://dx.doi.org/10.1126/science.aae0017.

Cummings, V., Hewitt, J., van Rooyen, A., Currie, K., Beard, S., Thrush, S., Norkko, J., Barr, N., Heath, P., Halliday, N.J., Sedcole, R., Gomez, A., McGraw, C., Metcalf, V., 2011. Ocean Acidification at High Latitudes: Potential Effects on Functioning of the Antarctic Bivalve Laternula elliptica. PLoS ONE 6(1), e16069. doi:10.1371/journal.pone.0016069

Delille, B., Jourdain, B., Borges, A.V., Delille, D., 2007. Biogas (CO_2, O_2, dimethylsulfide) dynamics in spring Antarctic fast ice. Limnol. Ocean. 52(4), 1367-1379.

Delille, B., Vancoppenolle, M., Geilfus, N., Tilbrook, B., Lannuzel, D., Schoemann, V., Becquevort, S., Carnat, G., Delille, D., Lancelot, C., Chou, L., Dieckmann, G.S., Tison, J.L., 2014. Southern Ocean CO_2 sink: The contribution of sea ice. J. Geophys. Res.-Oceans 119, 755 6340-6355. doi:10.1002/jgrc.20224.

Dickson, A.G., 1981. An exact definition of total alkalinity and a procedure for the estimation of alkalinity and total inorganic carbon from titration data. Deep-Sea Res. 28, 609-623.

Dickson, A.G., Millero, F.J., 1987. A comparison of the equilibrium constants for the dissociation of carbonic acid in seawater media. Deep-Sea Res. 34, 1733-1743.

Dickson, A.G., Sabine, C, Christian, J.R., 2007. Guide to best practices for ocean CO_2 measurements. PICES Special Publication 3, 191 pp.

Dieckmann, G.S., Nehrke, G., Papadimitriou, S., Göttlicher, J., Steininger, R., Kennedy, H., Wolf-Gladrow, D., Thomas, D.N., 2008. Calcium carbonate as ikaite crystals in Antarctic sea ice. Geophys. Res. Lett. 35, L08501. doi:10.1029/2008GL033540.

Dierssen, H.M., Smith, R.C., Vernet, M., 2002. Glacial meltwater dynamics in coastal waters west of the Antarctic Peninsula. Proc. Nat. Acad. Sci. 99, 1790-1795. doi: 10.1073/pnas.032206999.

Dlugokencky, E., Lang, P., Masarie, K., Crotwell, A.M., and Crotwell, M.J., 2014. Atmospheric Carbon Dioxide Dry Air Mole Fractions from the NOAA ESRL Carbon Cycle Cooperative Global Air Sampling Network, 1968-2013. available at: http://www.esrl.noaa.gov/gmd/ccgg/trends, last access: 28 January 2016.

Doney, S.C., Fabry, V.J., Feely, R.A., Kleypas, J.A., 2009. Ocean acidification: The other CO_2 problem, Annu. Rev. Mar. Sci., 1, 169–192, doi:10.1146/annurev.marine.010908.163834.

Ducklow, H.W., Baker, K., Martinson, D. G., Quetin, L. B., Ross, R. M., Smith, R. C., Stammerjohn, S. E., Vernet, M., Fraser, W., 2007. Marine pelagic ecosystems: the West Antarctic Peninsula. Phil. Trans. Royal Soc. B 362, 67-94. doi:10.1098/rstb.2006.1955.

Ducklow, H.W., Fraser, W., Meredith, M., Stammerjohn, S., Doney, S., Martinson, D., Sailley, S., Schofield, O., Steinberg, D., Venables, H., Amsler, C., 2013. West Antarctic Peninsula: An Ice-Dependent Coastal Marine Ecosystem in Transition. Oceanography 26, 190-203. doi:10.5670/oceanog.2013.62.

Egleston, E.S., Sabine, C.L., Morel, F.M.M., 2010. Revelle revisited: Buffer factors that quantify the response of ocean chemistry to changes in DIC and alkalinity. Glob. Biogeochem. Cycles 24, 1-9. doi:10.1029/2008GB003407.

Ericson, J., Lamare, M.D., Morely, S.A., Barker, M.F., 2010. The response of two ecologically important Antarctic invertebrates (Sterechinus neumayeri and Parborlasia corrugatus) to reduced seawater pH: effects on fertilisation and embryonic development. Mar. Biol. doi:10.1007/s00227-010-1529-y.

Evans, W., Mathis, J.T., Cross, J.N., 2014. Calcium carbonate corrosivity in an Alaskan inland sea. Biogeosciences 11, 363-379, 413. doi:10.5194/bg-11-365-2014.

Eveleth, R., Cassar, N., Doney, S.C., Munro, R., Sweeney, C., Biological and physical controls on O_2/Ar, Ar and pCO_2 variability at the Western Antarctic Peninsula and in the Drake Passage. Deep-Sea Res. II (2016), http://dx.doi.org/10.1016/j.dsr2.2016.05.002.

Fabry, V. J., Seibel, B.A., Feely, R.A., Orr, J.C., 2008. Impacts of ocean acidification on marine fauna and ecosystem processes, ICES J. Mar. Sci., 65, 414-432, doi:10.1093/icesjms/fsn048.

Feely, R.A., Sabine, C.L., Lee, K., Berelson, W., Kleypas, J., Fabry, V.J., Millero, F.J., 2004. Impact of Anthropogenic CO_2 on the $CaCO_3$ System in the Oceans. Science 305, 362-366. doi:10.1126/science.1097329.

Feely, R.A., Sabine, C.L., Hernandez-Ayon, J.M., Ianson, D., Hales, B., 2008. Evidence for upwelling of corrosive ‘‘acidified’’ water onto the continental shelf, Science, 320, 1490-1492, doi:10.1126/science.1155676.

Fransson, A., Chierici, M., Yager, P.L., Smith, W.O., 2011. Antarctic sea ice carbon dioxide system and controls. J. Geophys. Res. 116, C12035. doi:10.1029/2010JC006844.

Gerringa, L.J.A., Alderkamp, A-C., Laan, P., Thuroczy, C-E., de Baar, H.J.W., Mills, M.M., van Dijken, G.L., van Haren, H., Arrigo, K.R., 2012. Iron from melting glaciers fuels the phytoplankton blooms in Amundsen Sea (Southern Ocean): Iron biogeochemistry. Deep-Sea Res. II 71-76, 16-31.

Gibson, J.A.E., Trull, T.W., 1999. Annual cycle of fCO_2 under sea-ice and in open water in Prydz Bay, East Antarctica. Mar. Chem. 66, 187-200. doi:10.1016/S0304-4203(99)00040-7.

Geilfus, N.-X., Carnat, G., Papakyriakou, T., Tison, J.-L., Else, B., Thomas, H., Shadwick., E., Delille, B., 2012. Dynamics of pCO_2 and related air-ice CO_2 fluxes in the Arctic coastal zone (Amundsen Gulf, Beaufort Sea). J. Geophys. Res. 117, C00G10. doi:10.1029/2011JC007118.

Hauri, C., Doney, S.C., Takahashi, T., Erickson, M., Jiang, G., Ducklow, H.W., 2015. Two decades of inorganic carbon dynamics along the Western Antarctic Peninsula. Biogeosciences 12, 6761-6779. doi:10.5194/bgd-12-6929-2015.

Hartman, B., Hammond, D.E., 1985. Gas exchange in San Francisco Bay. Hydrobiologia 129, 59-68.

Henley, S.F., Tuerena, R.E., Annett, A.L., Fallick, A.E., Meredith, M.P., Venables, H.J., Clarke, A., Ganeshram, R.S., Macronutrient supply, uptake and recycling in the coastal ocean of the west Antarctic Peninsula. Deep-Sea Res. II (2016), http://dx.doi.org/10.1016/j.dsr2.2016.10.003.

Johnson, K.M., Sieburth, J.M., Williams, P.J.L., Brandstrom, L., 1987. Coulometric total carbon dioxide analysis for marine studies - automation and calibration. Mar. Chem. 21, 117-133.

Jones, E.M., Bakker, D.C.E., Venables, H.J., Hardman-Mountford, N., 2015. Seasonal cycle of CO_2 from the sea ice edge to island blooms in the Scotia Sea, Southern Ocean. Mar. Chem. 177, 490-500. http://dx.doi.org/10.1016/j.marchem.2015.06.031.

Jones, E.M., Bakker, D.C.E., Venables, H.J., Whitehouse, M.J., Korb, R.E., Watson, A.J., 2010. Rapid changes in surface water carbonate chemistry during Antarctic sea ice melt. Tellus B 62, 621-635. doi 10.1111/j.1600-0889.2010.00496.x.

Klinck, J.M., 1998. Heat and salt changes on the continental shelf west of the Antarctic Peninsula between January 1993 and January 1994. J. Geophys. Res.-Oceans 103(C4), 7617–7636. http://dx.doi.org/10.1029/98jc00369.

Klinck, J.M., Dinniman, M.S., 2010. Exchange across the shelf break at high southern latitudes. Ocean Sci. 6, 513-524. doi:10.5194/os-6-513-2010.

Klinck, J.M., Hofmann, E.E., Beardsley, R.C., Salihoglu, B., Howard, S., 2004. Watermass properties and circulation on the west Antarctic Peninsula Continental Shelf in Austral Fall and Winter 2001. Deep-Sea Res. II 51 (17-19), 1925-1946. http://dx.doi.org/10.1016/j.dsr2.2004.08.001.

Legge, O.J., Bakker, D.C.E., Meredith, M., Venables, H.J., Brown, P.J., Jones, E.M., Johnson, M.T., 2016. The seasonal cycle of carbonate system processes in Ryder Bay, West Antarctic Peninsula. Deep-Sea Res. II (2016), http://dx.doi.org/10.1016/j.dsr2.2016.11.006.

Legge, O.J., Bakker, D.C.E., Johnson, M.T., Meredith, M.P., Venables, H.J., Brown, P.J., Lee, G.A., 2015. The seasonal cycle of ocean-atmosphere CO_2 flux in Ryder Bay, west Antarctic Peninsula. Geophys. Res. Lett. 42, 2934-2942. doi:10.1002/2015GL063796.

Lewis, E., Wallace, D.W.R., 1998. CO2SYS-Program developed for the CO_2 system calculations. Carbon Dioxide Information and Analysis Centre. Report ORNL/CDIAC-105.

Martinson, D.G., Stammerjohn, S.E., Iannuzzi, R.A., Smith, R.C., Vernet, M., 2008. Western Antarctic Peninsula physical oceanography and spatio-temporal variability. Deep-Sea Res. II 55, 1964-1987. http://dx.doi.org/10.1016/j.dsr2.2008.04.038.

Martinson, D.G., McKee, D.C., 2012. Transport of warm upper circumpolar deep water onto the western Antarctic Peninsula continental shelf. Ocean Sci. 8 (4), 433-442. http://dx.doi.org/10.5194/os-8-433-2012.

Mattsdotter Björk, M., Fransson, A., Torstensson, A., Chierici, M., 2014. Ocean acidification state in western Antarctic surface waters: controls and interannual variability. Biogeosciences 11, 57-73. doi:10.5194/bg-11-57-2014.

McClintock, J.B., Robert, A., Angus, R.A., Mcdonald, M.R., Amsler, C.D., Catledge, S.A., Vohra, Y.K., 2009. Rapid dissolution of shells of weakly calcified Antarctic benthic macroorganisms indicates high vulnerability to ocean acidification. Ant. Sci. 21(5), 449-456. doi: https://doi.org/10.1017/S0954102009990198.

McNeil, B.I., Matear, R.J., 2008. Southern Ocean acidification: a tipping point at 450-ppm atmospheric CO_2. Proc. Nat. Acad. Sci. 105, 18860-18864. doi:10.1073/pnas.0806318105.

McNeil, B.I., Sweeney, C., Gibson, J.A.E., 2011. Short Note: Natural seasonal variability of aragonite saturation state within two Antarctic coastal ocean sites. Ant. Sci. 23, 411-412. doi:10.1017/S0954102011000204.

Mehrbach, C., Culberson, C.H., Hawley, J.E., Pytkowicz, R.M., 1973. Measurement of the apparent dissociation constants of carbonic acid in seawater at atmospheric pressure. Limnol. Ocean. 18, 897-907.

Meredith, M.P., Renfrew, I.A., Clarke, A., King, J.C., Brandon, M.A., 2004. Impact of the 1997/98 ENSO on upper ocean characteristics in Marguerite Bay, western Antarctic Peninsula. J. Geophys. Res. 109, C09013. doi:10.1029/2003JC001784.

Meredith, M.P., King, J.C., 2005. Rapid climate change in the ocean west of the Antarctic Peninsula during the second half of the 20th century. Geophys. Res. Lett. 32, L19604. doi:10.1029/2005GL024042.

Meredith, M.P., Brandon, M.A., Wallace, M.I., Clarke, A., Leng, M.J., Renfrew, I.A., van Lipzig, N.P.M., King, J.C., 2008. Variability in the freshwater balance of northern Marguerite Bay, Antarctic Peninsula: Results from $\delta^{18}O$. Deep-Sea Res. II 55, 309-322. doi:10.1016/j.dsr2.2007.11.005.

Meredith, M.P., Wallace, M.I., Stammerjohn, S.E., Renfrew, I.A., Clarke, A., Venables, H.J., Shoosmith, D.R., Souster, T., Leng, M.J., 2010. Changes in the freshwater composition of the upper ocean west of the Antarctic Peninsula during the first decade of the 21st century. Prog. Ocean. 87, 127-143. doi:10.1016/j.pocean.2010.09.019.

Meredith, M.P., Venables, H.J., Clarke, A., Ducklow, H.W., Erickson, M., Leng, M.J., Lenaerts, J.T.M., and van den Broeke, M.R., 2013. The Freshwater System West of the Antarctic Peninsula: spatial and temporal changes, J. Climate 26, 1669-1684. doi:10.1175/JCLI-D-25 12-00246.1, 2013.

Millero, F.J., 2007. The marine inorganic carbon cycle, Chem. Rev. 107, 308-341. doi:10.1021/cr0503557.

Mitchell R.G., Holm-Hansen, O., 1991. Observations and modelling of the Antarctic phytoplankton crop in relation to mixing depth. Deep-Sea Res. 38, 981-1007.

Moffat, C., Beardsley, R.C., Owens, B., van Lipzig, N., 2008. A first description of the Antarctic Peninsula Coastal Current. Deep-Sea Res Part II 55 (3-4), 277-293. http://dx.doi.org/10.1016/j.dsr2.2007.10.003.

Moffat, C., Owens, B., Beardsley, R.C., 2009. On the characteristics of Circumpolar Deep Water intrusions to the west Antarctic Peninsula Continental Shelf. J Geophys Res.-Oceans 114. http://dx.doi.org/10.1029/2008jc004955.

Montes-Hugo, M., Doney, S.C., Ducklow, H.W., Fraser, W., Martinson, D., Stammerjohn, S.E., Schofield, O., 2009. Recent changes in phytoplankton communities associated with rapid regional climate change along the western Antarctic Peninsula, Science 323, 1470-1473. doi:10.1126/science.1164533.

Montes-Hugo, M., Sweeney, C., Doney, S.C., Ducklow, H.W., Frouin, R., Martinson, D.G., Stammerjohn, S., Schofield, O., 2010. Seasonal forcing of summer dissolved inorganic carbon and chlorophyll a on the western shelf of the Antarctic Peninsula, J. Geophys. Res. 115, C03024, doi:10.1029/2009JC005267.

Morely, S.A., Hirse, T., Pörtner, H.-O., Peck, L.S., 2009. Geographic variation in thermal tolerance within Southern Ocean marine ectotherms. Comp. Biochem. Physiol. A 153, 154-161.

Mosby, H., 1934. The waters of the Atlantic Antarctic Ocean. Kommisjon hos Jacob Dybwad, Oslo, (131pp).

Moy, A.D., Howard, W.R., Bray, S.G., Trull, T.W., 2009. Reduced calcification in modern Southern Ocean planktonic foraminifera. Nat. Geosci. Lett., doi:10.1038/NGEO460.

Mucci, A., 1983. The solubility of calcite and aragonite in seawater at various salinities, temperatures, and one atmosphere total pressure. Am. J. Sci. 283, 780-799.

Neven, I.A., Stefels, J., van Heuven, S.M.A.C., de Baar, H.J.W., Elzenga, J.T.M., 2011. High plasticity in inorganic carbon uptake by Southern Ocean phytoplankton in response to ambient CO_2. Deep-Sea Res. II 58, 2636-2646. doi:10.1016/j.dsr2.2011.03.006.

Orr, J.C., Fabry, V.J., Aumont, O., Bopp, L., Doney, S.C., Feely, R.A., Gnanadesikan, A., Gruber, N., Ishida, A., Joos, F., Key, R.M., Lindsay, K., Maier-Reimer, E., Matear, R., Monfray, P., Mouchet, A., Najjar, R.G., Plattner, G.K., Rodgers, K.B., Sabine, C.L., Sarmiento, J.L., Schlitzer, R., Slater, R.D., Totterdell, I.J., Weirig, M.F., Yamanaka, Y., Yool, A., 2005. Anthropogenic ocean acidification over the twenty-first century and its impact on calcifying organisms. Nature 437, 681-686. doi:10.1038/nature04095.

Papadimitriou, S., Kennedy, H., Kattner, G., Dieckmann, G., Thomas, D., 2004. Experimental evidence for carbonate precipitation and CO_2 degassing during sea ice formation, Geochim. Cosmochim. Acta 68, 1749-1761. doi:10.1016/j.gca.2003.07.004.

Prezelin, B.B., Hofmann, E.E., Mengelt, C., Klinck, J.M., 2000. The linkage between Upper Circumpolar Deep Water (UCDW) and phytoplankton assemblages on the west Antarctic Peninsula continental shelf. J. Mar. Res. 58 (2), 165–202. http://dx.doi.org/10.1357/002224000321511133.

Pritchard, H.D., Ligtenberg, S.R.M., Fricker, H.A., Vaughan, D.G., van den Broeke, M.R., Padman, L., 2012. Antarctic ice-sheet loss driven by basal melting of ice shelves. Nature 484 (7395), 502–505. http://dx.doi.org/10.1038/Nature10968.

Roden, N.P., Shadwick, E.H., Tilbrook, B., Trull, T.W., 2013. Annual cycle of carbonate chemistry and decadal change in coastal Prydz Bay, East Antarctica. Mar. Chem. 155, 135-147. doi:10.1016/j.marchem.2013.06.006.

Royal Society, 2005. Ocean acidification due to increasing atmospheric carbon dioxide, report, Clyvedon Press, Cardiff, U. K.

Rysgaard, S., Glud, R.N., Sejr, M.K., Bendtsen, J., Christensen, P.B., 2007. Inorganic carbon transport during sea ice growth and decay: A carbon pump in polar seas. J. Geophys. Res. 112, C03016. doi:10.1029/2006JC003572.

Rysgaard, S., Glud, R.N., Lennert, K., Cooper, M., Halden, N., Leakey, R.J.G., Hawthorne, F.C., Barber, D., 2012. Ikaite crystals in melting sea ice implications for pCO_2 and pH levels in Arctic surface waters, Cryosphere 6, 901-908. doi:10.5194/tc-6-901-2012.

Sasse, T.P., McNeil, B.I., Matear, R.J., Lenton, A., 2015. Quantifying the influence of CO_2 seasonality on future aragonite undersaturation onset. Biogeosciences 12, 6017-6031. doi:10.5194/bg-12-6017-2015.

Sabine, C.L., Feely, R.A., Gruber, N., Key, R.M., Lee, K., Bullister, J.L., Wanninkhof, R., Wong, C.S., Wallace, D.W.R., Tilbrook, B., Millero, F.J., Peng, T.h., Kozyr, A., 2004. The Oceanic Sink for Anthropogenic CO_2. Science 305, 367-371. doi:10.1126/science.1097403.

Shadwick, E.H., Thomas, H., Chierici, M., Else, B., Fransson, A., Michel, C., Miller, L.A., Mucci, A., Niemi, A., Papakyriakou, T.N., Tremblay, J.-E., 2011. Seasonal variability of the inorganic carbon system in the Amundsen Gulf region of the southeastern Beaufort Sea. Limnol. Oceanogr., 56(1), 303-322. doi:10.4319/lo.2011.56.1.0303

Shadwick, E.H., Trull, T.W., Thomas, H., Gibson, J.A.E., 2013. Vulnerability of polar oceans to anthropogenic acidification: comparison of Arctic and Antarctic seasonal cycles. Scientific reports 3, 2339. doi:10.1038/srep02339.

Smith, D.A., Hofmann, E.E., Klinck, J.M., Lascara, C.M., 1999. Hydrography and circulation of the west Antarctic Peninsula continental shelf. Deep-Sea Res. I 46 (6), 925–949. http://dx.doi.org/10.1016/S0967-0637(98)00103-4.

Smith, W.O., Nelson, D.M., 1985. Phytoplankton Bloom Produced by a Receding Ice Edge in the Ross Sea - Spatial Coherence with the Density Field. Science 227 (4683), 163-166. http://dx.doi.org/10.1126/science.227.4683.163.

Stammerjohn, S.E., Martinson, D.G., Smith, R.C., Iannuzzi, R.A., 2008. Sea ice in the western Antarctic Peninsula region: spatio-temporal variability from ecological and climate change perspectives. Deep-Sea Res. II 55, 2041-2058.

Stammerjohn, S.E., Massom, R., Rind, D., Martinson, D., 2012. Regions of rapid sea ice change: an inter-hemispheric seasonal comparison. Geophys. Res. Lett. 39 (6), L06501. http://dx.doi.org/10.1029/2012GL050874.

Steinacher, M., Joos, F., Frölicher, T.L., Plattner, G.-K., Doney, S.C., 2009. Imminent ocean acidification in the Arctic projected with the NCAR global coupled carbon cycle-climate model. Biogeosciences 6, 515-533. doi:10.5194/bg-6-515-2009.

Stukel, M.R., Asher, E., Couto, N., Schofield, O., Strebel, S., Tortell, P., Ducklow, H.W., 2015. The imbalance of new and export production in the western Antarctic Peninsula, a potentially “leaky” ecosystem, Global Biogeochem. Cycles 29, 1400-1420, doi:10.1002/2015GB005211.

Sweeney, C. 2003. The annual cycle of surface CO_2 and O_2 in the Ross Sea: a model for gas exchange on the continental shelves of Antarctica. Antarctic Research Series, 78, 295-312.

Takahashi, T., Sutherland, S.C., Wanninkhof, R., Sweeney, C., Feely, R.A., Chipman, D.W., Hales, B., Friederich, G., Chavez, F., Sabine, C.L., Watson, A.J., Bakker, D.C.E., Schuster, U., Metzl, Yoshikawa-Inoue, H., Ishii, M., Midorikawa, T., Nojiri, Y., Körtzinger, Steinhoff, T., Hoppema, M., Olafsson, J., Arnarson, T.S., Tilbrook, B., Johannessen, T., Olsen, A., Bellerby, R., Wong, C.S., Delille, B., Bates, N.R., de Baar, H.J.W., 2009. Climatological mean and decadal change in surface ocean pCO_2, and net sea-air CO_2 flux over the global oceans. Deep-Sea Res. II 56, 554-577.

Takahashi, T., Sutherland, S.C., Chipman, D.W., Goddard, J.G., Ho, C., Newberger, T., Sweeney, C., Munro, D.R., 2014. Climatological distributions of pH, pCO_2, total CO_2, alkalinity, and $CaCO_3$ saturation in the global surface ocean, and temporal changes at selected locations. Mar. Chem. 164, 95-125.

Takahashi, T., Sutherland, S. C., and Kozyr, A.: Global ocean surface water partial pressure of CO2 database: measurements performed during 1957-2012 (Version 2012), ORNL/CDIAC- 160, NDP-088(V2012), Carbon Dioxide Inf. Anal. Center, Oak Ridge Natl. Lab. U.S. Dep. Energy, Oak Ridge, Tennessee, doi:10.3334/CDIAC/OTG.NDP088(V2012), 2015.

Tortell, P.D., Bittig, H.C., Körtzinger, A., Jones, E.M., Hoppema, M., 2015. Biological and physical controls on N_2, O_2, and CO_2 distributions in contrasting Southern Ocean surface waters. Glob. Biogeochem. Cycles 29, 994-1013. doi:10.1002/2014GB004975.

Trimborn, S., Brenneis, T., Sweet, E., Rost, B., 2013. Sensitivity of Antarctic phytoplankton species to ocean acidification: Growth, carbon acquisition, and species interaction. Limnol. Oceanogr. 58(3), 997-1007. doi:10.4319/lo.2013.58.3.0997.

Tynan, E., Clarke, J.S., Humphreys, M.P., Ribas-Ribas, M., Esposito, M., Rérolle, V.M.C., Schlosser, C., Thorpe, S.E., Tyrrell, T., Achterberg, E.P., 2016. Physical and biogeochemical controls on the variability in surface pH and calcium carbonate saturation states in the Atlantic sectors of the Arctic and Southern Oceans. Deep-Sea Res. II 127, 7-27.

van Heuven, S., Pierrot, D., Rae, J., Lewis, E., Wallace, D., 2011. MATLAB Program Developed for CO_2 System Calculations, ORNL/CDIAC-105b, Carbon Dioxide Information Analysis Center, Oak Ridge National Laboratory, U.S. Department of Energy, Oak Ridge, Tennessee. doi:10.3334/CDIAC/otg.CO2SYS.

Vaughan, D.G., Marshall, G.J., Connolley, W.M., Parkinson, C., Mulvaney, R., Hodgson, D.A., King, J.C., Pudsey, C.J., Turner, J., 2003. Recent rapid regional climate warming on the Antarctic Peninsula. Climatic Change 60, 243-274. doi:10.1023/A:1026021217991.

Venables, H.J., Clarke, A., Meredith, M.P., 2013. Wintertime controls on summer stratification and productivity at the western Antarctic Peninsula. Limnology and Oceanography 58, 1035-1047. doi:10.4319/lo.2013.58.3.1035.

Venables, H.J., Meredith, M.P., 2014. Feedbacks between ice cover, ocean stratification, and heat content in Ryder Bay, West Antarctic Peninsula. J. Geophys. Res.-Oceans 119, 5323-5336. doi:10.1002/jgrc.20224.

Venables, H.J., Meredith, M.P., Brearley, J.A., Modification of deep waters in Marguerite Bay, western Antarctic Peninsula, caused by topographic overflows. Deep-Sea Res. II (2016), http://dx.doi.org/10.1016/j.dsr2.2016.09.005.

Vernet, M., Martinson, D., Iannuzzi, R., Stammerjohn, S., Kozlowski, W., Sines, K., Smith, R., and Garibotti, I., 2008. Primary production within the sea-ice zone west of the Antarctic Peninsula: sea ice, summer mixed layer, and irradiance. Deep-Sea Res. II 55, 2068-2085, doi:10.1016/j.dsr2.2008.05.021.

Wallace, M.J., Meredith, M.P., Brandon, M. A., Sherwin, T.J., Dale, A., Clarke, A., 2008. On the characteristics of internal tides and coastal upwelling behaviour in Marguerite Bay, west Antarctic Peninsula. Deep-Sea Res. II 55, 2023-2040.

Weston, K., Jickells, T.D., Carson, D.S., Clarke, A., Meredith, M.P., Brandon, M.A., Wallace, M.I., Ussher, S.J., Hendry, K.R., 2013. Primary production export flux in Marguerite Bay (Antarctic Peninsula): Linking upper water-column production to sediment trap flux. Deep-Sea Res. I 75, 52-66. doi:10.1016/j.dsr.2013.02.001.

Wang, X., Yang, G.-P., López, D., Ferreyra, G., Lemarchand, K., Xie, H., 2009. Late autumn to spring changes in the inorganic and organic carbon dissolved in the water column at Scholaert Channel, West Antarctica, Antarctic Science 22, 145. doi:10.1017/S0954102009990666.

Wanninkhof, R., Park, G.H., Takahashi, T., Sweeney, C., Feely, R., Nojiri, Y., Gruber, N., Doney, S.C., McKinley, G.A., Lenton, A., Le Quéré, C., Heinze, C., Schwinger, J., Graven, H., Khatiwala, S., 2013.

Global ocean carbon uptake: magnitude, variability and trends. Biogeosciences 10, 1983-2000. doi:10.5194/bg-10-1983-2013.

Weiss, R.F., 1974. Carbon dioxide in water and seawater: The solubility of a non-ideal gas, Mar. Chem. 2, 203-215. doi:10.1016/0304-4203(74)90015-2.

Weiss, R.F., Price, B.A., 1980. Nitrous-Oxide Solubility in Water and Seawater. Mar. Chem. 8, 347-359.

Wolf-Gladrow, D.A., Zeebe, R.E., Klaas, C., Koertzinger, A., Dickson, A.G., 2007. Total alkalinity: The explicit conservative expression and its application to biogeochemical processes. Mar. Chem. 106 (1-2), 287-300. http://dx.doi.org/10.1016/j.marchem.2007.01.006.

Yamamoto-Kawai, M., Mclaughlin, F.A., Carmack, E.C., Nishino, S., Shimada, K., 2009. Aragonite Undersaturation in the Arctic Ocean: Effects of Ocean Acidification and Sea Ice Melt. Science 1098. doi:10.1126/science.1174190.

Zeebe, R., Wolf-Gladrow, D., 2001. CO_2 in Seawater: Equilibrium, Kinetics, Isotopes. Elsevier, Amsterdam.

Fig. 1. Map of the West Antarctic Peninsula (WAP) showing Adelaide Island, Marguerite Bay and Ryder Bay (insert). Sampling sites A, B, C, D, F, G, I, J, K, RaTS1, RaTS2, LMG1 (1), LMG2 (2) are marked by black dots. The locations of Rothera Research Station, Sheldon Glacier, Horton Glacier, Hurley Glacier, Lèoni Island and Lagoon Island are marked. General flow of the Antarctic Circumpolar Current is indicated along the WAP in the offshore Bellingshausen Sea region.

Fig. 2. Site locations in Ryder Bay (a) and sea surface distributions of (b) salinity; (c) potential temperature (θ, °C); (d) C_T (μmolkg^{-1}); (e) A_T (μmolkg^{-1}); (f) nitrate (NO_3, μmolkg^{-1}); (g) $pCO_{2\ AT\text{-}CT}$ (μatm); (h) pH_T; and (i) aragonite saturation state (Ωaragonite) across Ryder Bay. Ωaragonite is calculated at in-situ temperature and pressure. Sampling sites are marked by black dots.

Fig. 3. Site locations in Ryder Bay (a) and deep water distributions of (b) pH_T; and (c) aragonite saturation state (Ωaragonite) across Ryder Bay. Black dashed line in (c) shows the location of undersaturated (Ω <1) water. pH_T and Ωaragonite are calculated at in-situ temperature and pressure. Sampling sites are marked by black dots.

Fig. 4. (a) Potential temperature (θ, °C) versus salinity plot, related to aragonite saturation state (Ωaragonite); (b) relationship of A_T (upper line; $\mu molkg^{-1}$) and C_T (lower line; $\mu molkg^{-1}$) as a function of salinity, related to aragonite saturation state (Ωaragonite). Principle water masses are labelled in (a): Antarctic Surface Water (AASW), Winter Water (WW), and modified Circumpolar Deep Water (mCDW). Trend lines in (b) represent salinity-dilution using glacial ice endmember S = 0, C_T = 16 $\mu molkg^{-1}$, A_T = 100 $\mu molkg^{-1}$ (solid line) and sea-ice endmember S = 7, C_T = 277 $\mu molkg^{-1}$, A_T = 328 $\mu molkg^{-1}$ (dashed line) with S = 34.7, C_T = 2276 $\mu molkg^{-1}$, A_T = 2348 $\mu molkg^{-1}$ as the end member for mCDW (Smith et al., 1999). Ωaragonite is calculated at in-situ temperature and pressure.

Fig. 5. Site location in Ryder Bay showing upper (sites F, D, C, RaTS1, B, RaTS2, A) and lower (sites I, G, J, K) sections (a) and depth distributions of (b) A_T ($\mu molkg^{-1}$) upper section; (c) A_T ($\mu molkg^{-1}$) lower section; (d) C_T ($\mu molkg^{-1}$) upper section; (e) C_T ($\mu molkg^{-1}$) lower section; (f) aragonite saturation state (Ωaragonite) upper section; (f) aragonite saturation state (Ωaragonite) lower section. Ωaragonite is calculated at in-situ temperature and pressure. Sampling sites in Ryder Bay are marked by black dots and labelled in (a). Sampling depths in the water column are marked by black dots in (b-f).

Fig. 6. Relationship of (a) calcite saturation state (Ωcalcite) and aragonite saturation state (Ωaragonite) as a function of pH_T, related to salinity; (b) aragonite saturation state (Ωaragonite) as a function of salinity, related to water column depth; (c) aragonite saturation state (Ωaragonite) as a function of nitrate (NO_3; $\mu molkg^{-1}$) concentrations, related to salinity; and (d) aragonite saturation state (Ωaragonite) as a function of C_T ($\mu molkg^{-1}$) concentrations, related to salinity. Ωcalcite and Ωaragonite are calculated at in-situ temperature and pressure. Surface data (<10 m) highlighted with open black circles. The horizontal black-dashed line represents when saturation states are equal to 1 where data below the line represent carbonate mineral undersaturation.

Fig. 7. Relationship of potential alkalinity (A^*_T; $\mu mol\ kg^{-1}$) as a function of salinity for all data (grey dots) in the summer mixed layer AASW, sea surface data (<10 m) are highlighted with open black circles. The solid-black line represents the potential alkalinity-salinity linear regression trend A_T^* = 69.S + 2. The black-dashed lines represent hypothetical salinity-dilution lines using glacial ice endmember S = 0, A_T =

100 µmol kg^{-1} and sea-ice endmember S = 7, A_T = 328 µmol kg^{-1} and S = 34.7, A_T = 2348 µmolkg^{-1} as end members for mCDW (Smith et al., 1999).

Fig. 8. Sea surface pCO_2 ($pCO_{2\ ship}$; µatm) aboard ARSV Laurence M. Gould in the Marguerite Bay and Ryder Bay region during 18 January 2014. Data points are marked by black dots. Sites occupied for water column sampling (RaTS1, LMG1, LMG2) are marked by black circles and labelled.

Fig. 9. Depth profiles of (a) potential temperature (θ, °C); (b) salinity; (c) A_T (µmolkg^{-1}); and (d) C_T (µmolkg^{-1}) from all sites in Ryder Bay (grey dots) and Marguerite Bay (black dots).

Table 1. Ryder Bay and Marguerite Bay sampling sites; location; sampling date (2014); Δt (days) time from winter (t_0) 17 September 2013 until sampling date; water column depth (m); mixed layer depth (MLD, m); depth of potential temperature minimum (θ_{min}, m); AASW average aragonite saturation state (Ω); Winter Water average aragonite saturation state (Ω); mCDW average aragonite saturation state (Ω); ΔpCO_2 (µatm) from the difference between shipboard daily mean air pCO_2 and calculated seawater $pCO_{2\ AT\text{-}CT}$; CO_2 flux (mmol m^{-2} day^{-1}). Ω is calculated at in-situ temperature and pressure. Average values and standard deviations for all Ryder Bay data are shown beneath the respective variable. – means no data.

site	location	date	Δt	depth	MLD	θ_{min}	AASW Ω	WW Ω	mCDW Ω	ΔpCO_2	CO_2 flux
		dd-mm	days	m	m	m				µatm	mmol m^{-2} day^{-1}
RaTS 1	Ryder Bay coast	18-01	123	503	14.0	73.0	2.6	1.1	0.9	−228	−48.6
RaTS 2	Ryder Bay coast	29-01	134	340	2.5	49.5	3.0	1.0	0.9	−243	−49.3
A	Ryder Bay entrance	21-01	126	317	3.5	49.0	3.1	1.1	1.0	−256	−55.4
B	Ryder Bay coast	31-01	136	372	3.0	49.0	2.9	1.0	0.9	−243	−50.4
C	Ryder Bay coast	21-02	157	378	7.0	61.0	1.9	1.0	1.0	−162	−32.5
D	Ryder Bay sea ice	05-02	141	252	2.5	53.0	3.1	1.0	–	−254	−55.1
F	Sheldon Glacier	16-01	121	174	20.5	94.0	2.3	1.4	–	−202	−43.3

G	Ryder Bay centre	19-02	155	136	19.5	76.0	1.9	1.0	–	−145	−29.8
I	Horton-Hurley Glaciers	28-01	133	184	5.0	52.0	3.1	1.0	–	−242	−48.1
J	Léoni-Lagoon Islands	12-02	148	300	10.5	52.0	2.2	1.1	–	−176	−34.7
K	Lagoon Island	01-03	165	94	48.5	87.5	1.8	1.4	–	−133	−27.9
						average	2.5±0.5	1.1±0.2	0.9±0.0	−208±46	−43.2±10.2
LMG1	Marguerite Bay	18-01	123	584	7.0	49.0	2.7	1.0	1.0	−226	−44.9
LMG2	Marguerite Bay	18-01	123	475	10.0	52.0	2.4	1.0	1.0	−197	−41.7

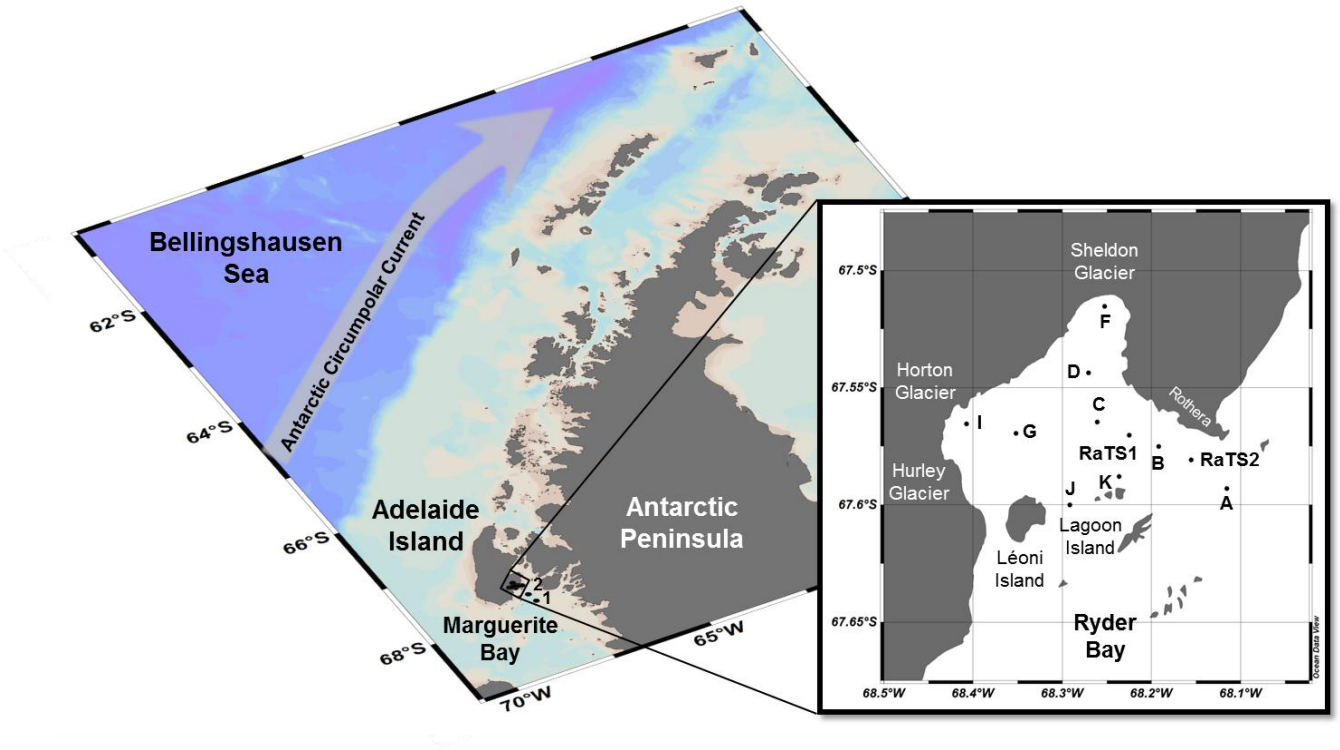

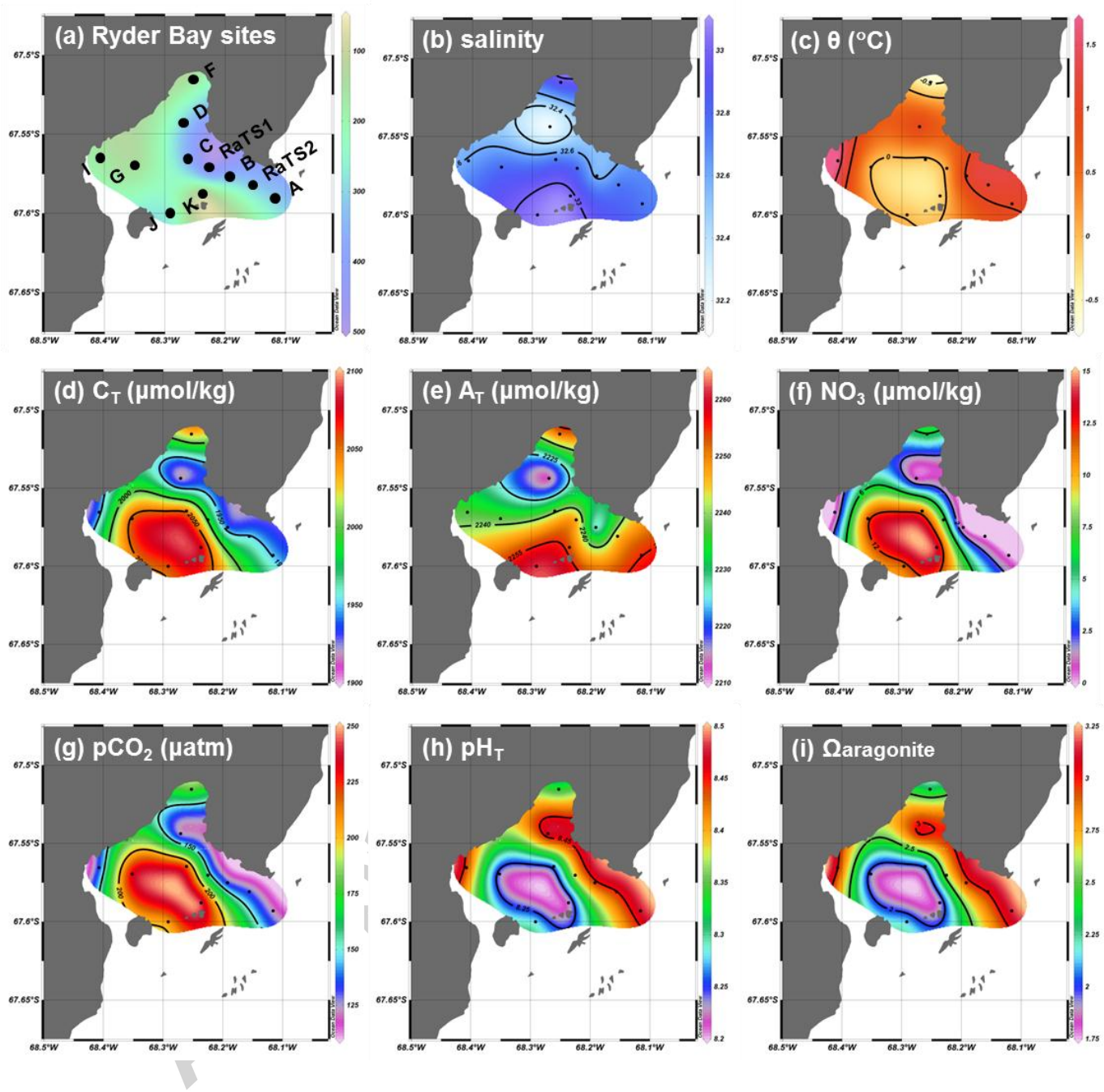
(a) Ryder Bay sites
F
D
C
RaTS1
B
RaTS2
A
K
J
G
I
(b) salinity
(c) θ (°C)
(d) C_T (µmol/kg)
(e) A_T (µmol/kg)
(f) NO_3 (µmol/kg)
(g) pCO_2 (µatm)
(h) pH_T
(i) Ωaragonite
67.5°S
67.55°S
67.6°S
67.65°S
68.5°W
68.4°W
68.3°W
68.2°W
68.1°W

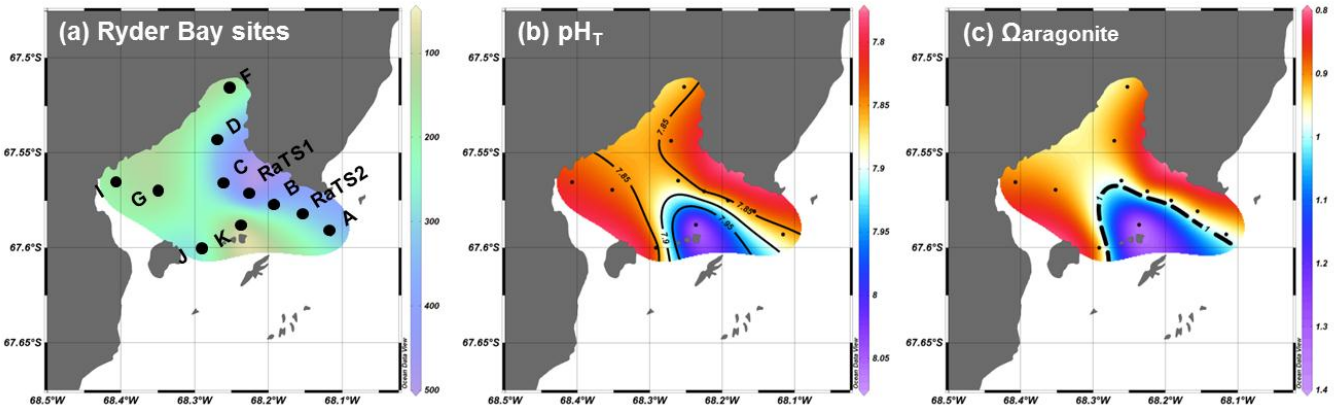
(a) Ryder Bay sites
F
D
C
RaTS1
B
RaTS2
A
I
G
J
K
(b) pH$_T$
(c) Ωaragonite
67.5°S
67.55°S
67.6°S
67.65°S
68.5°W
68.4°W
68.3°W
68.2°W
68.1°W

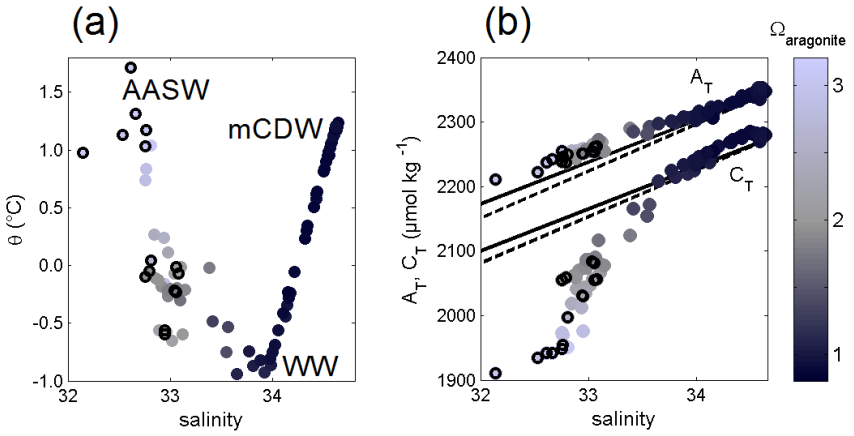
(a)
AASW
mCDW
WW
θ (°C)
salinity
(b)
$\Omega_{aragonite}$
A_T
C_T
A_T, C_T (μmol kg^{-1})
salinity

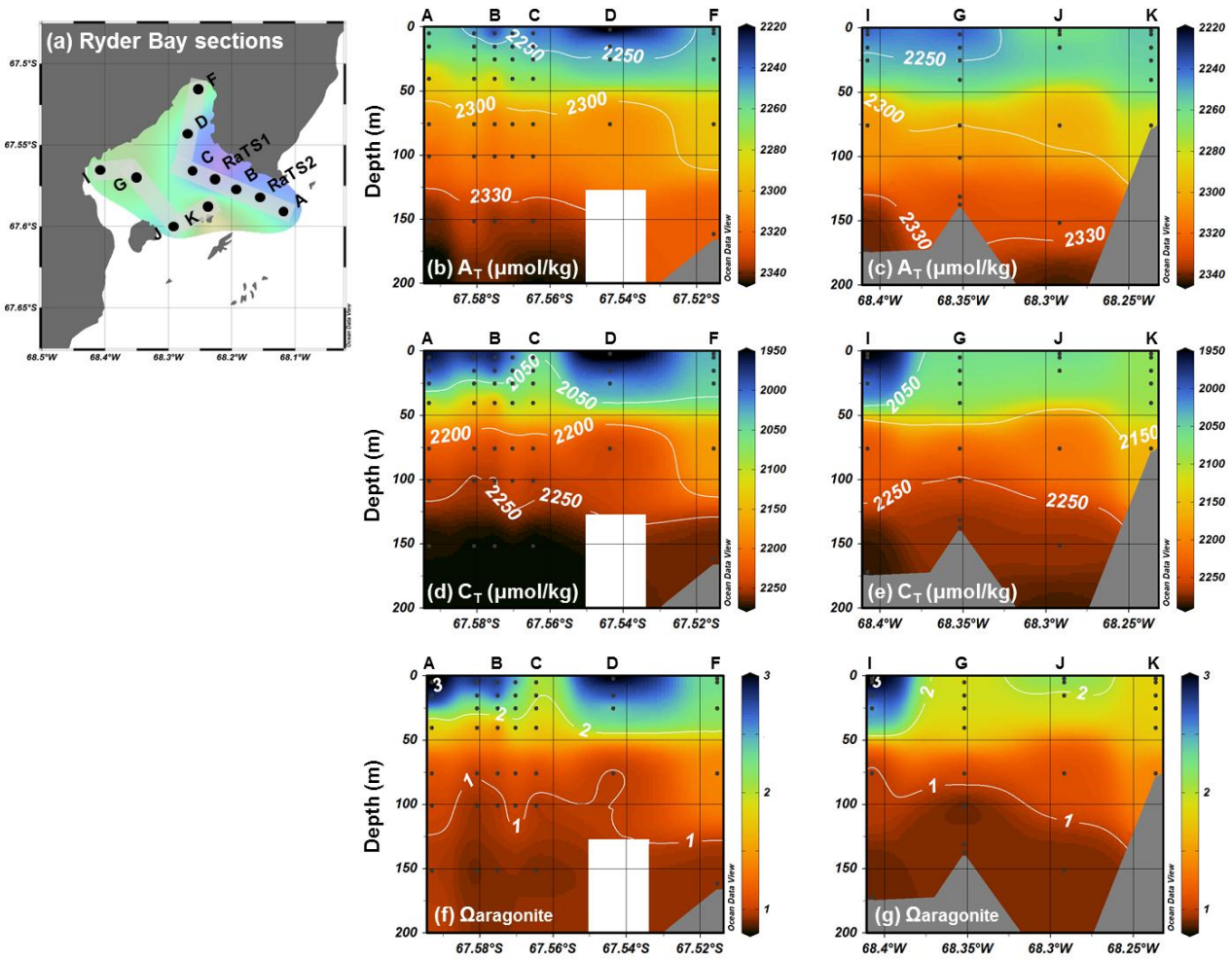
(a) Ryder Bay sections
RaTS1
RaTS2
(b) A_T (µmol/kg)
(c) A_T (µmol/kg)
(d) C_T (µmol/kg)
(e) C_T (µmol/kg)
(f) Ωaragonite
(g) Ωaragonite
Depth (m)
Ocean Data View

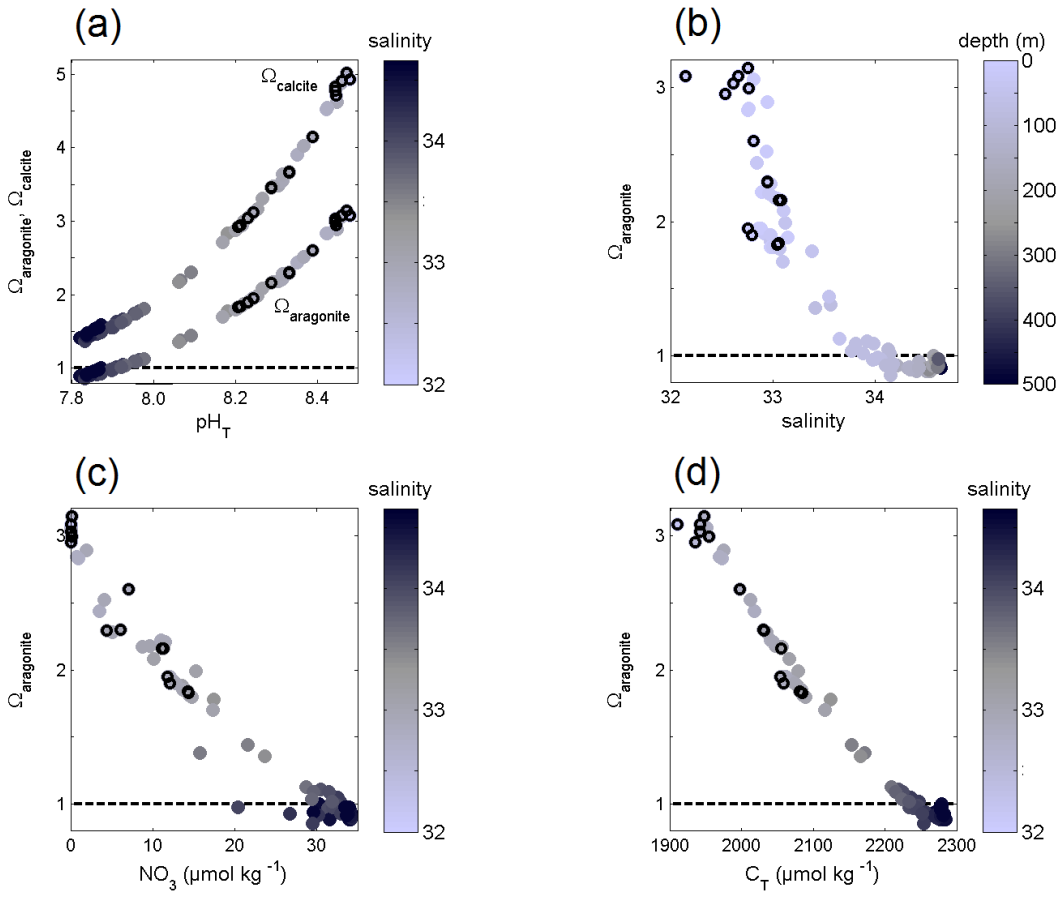
(a)
salinity
$\Omega_{calcite}$
$\Omega_{aragonite}$
$\Omega_{aragonite}$, $\Omega_{calcite}$
pH_T
(b)
depth (m)
$\Omega_{aragonite}$
salinity
(c)
salinity
$\Omega_{aragonite}$
NO_3 (µmol kg $^{-1}$)
(d)
salinity
$\Omega_{aragonite}$
C_T (µmol kg $^{-1}$)

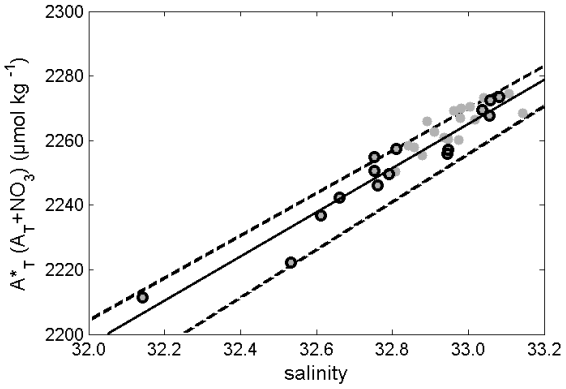
2300
2280
2260
2240
2220
2200
32.0
32.2
32.4
32.6
32.8
33.0
33.2
salinity
A*T (AT+NO3) (µmol kg-1)

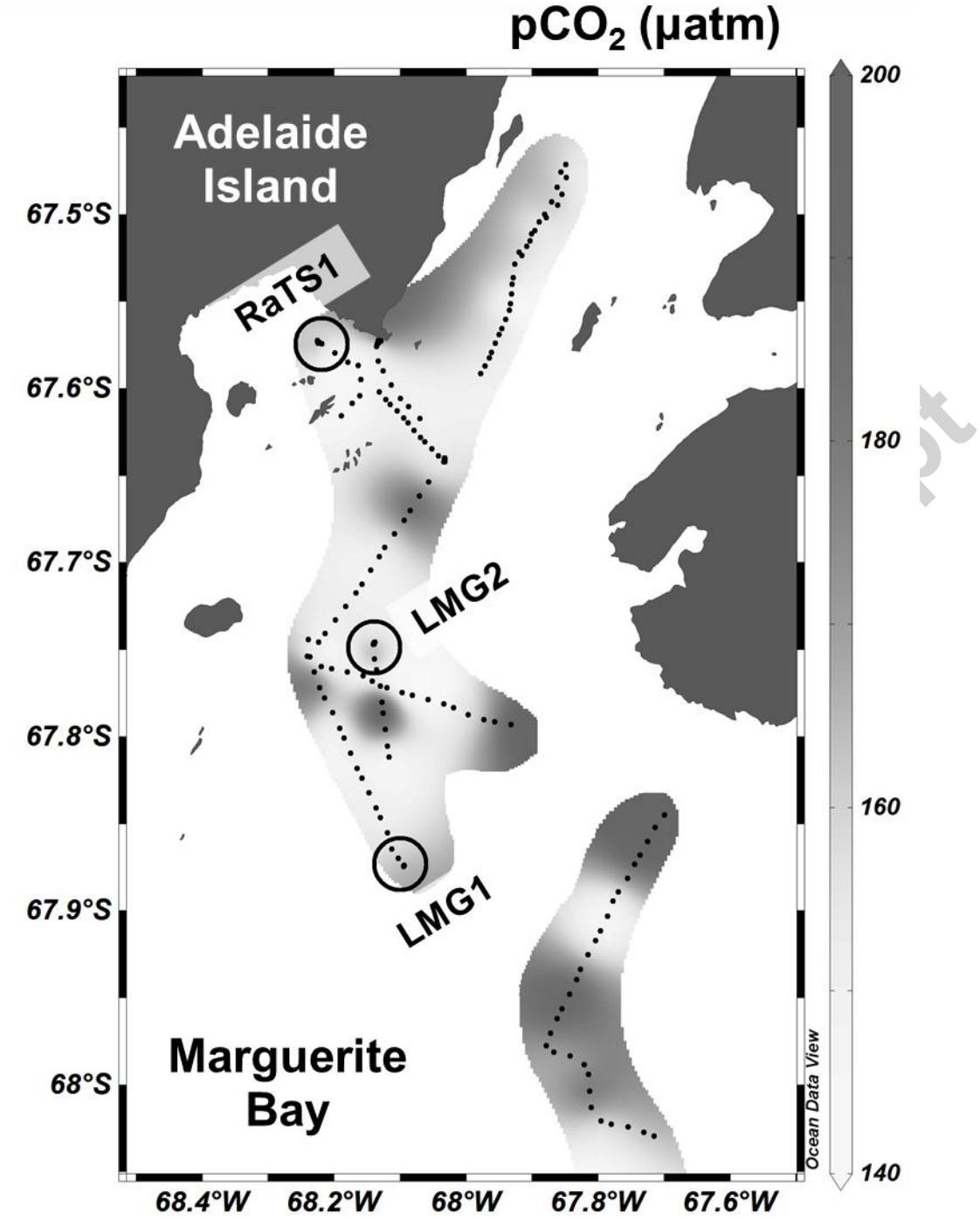
pCO2 (µatm)
200
180
160
140
Adelaide Island
RaTS1
LMG2
LMG1
Marguerite Bay
67.5°S
67.6°S
67.7°S
67.8°S
67.9°S
68°S
68.4°W
68.2°W
68°W
67.8°W
67.6°W
Ocean Data View

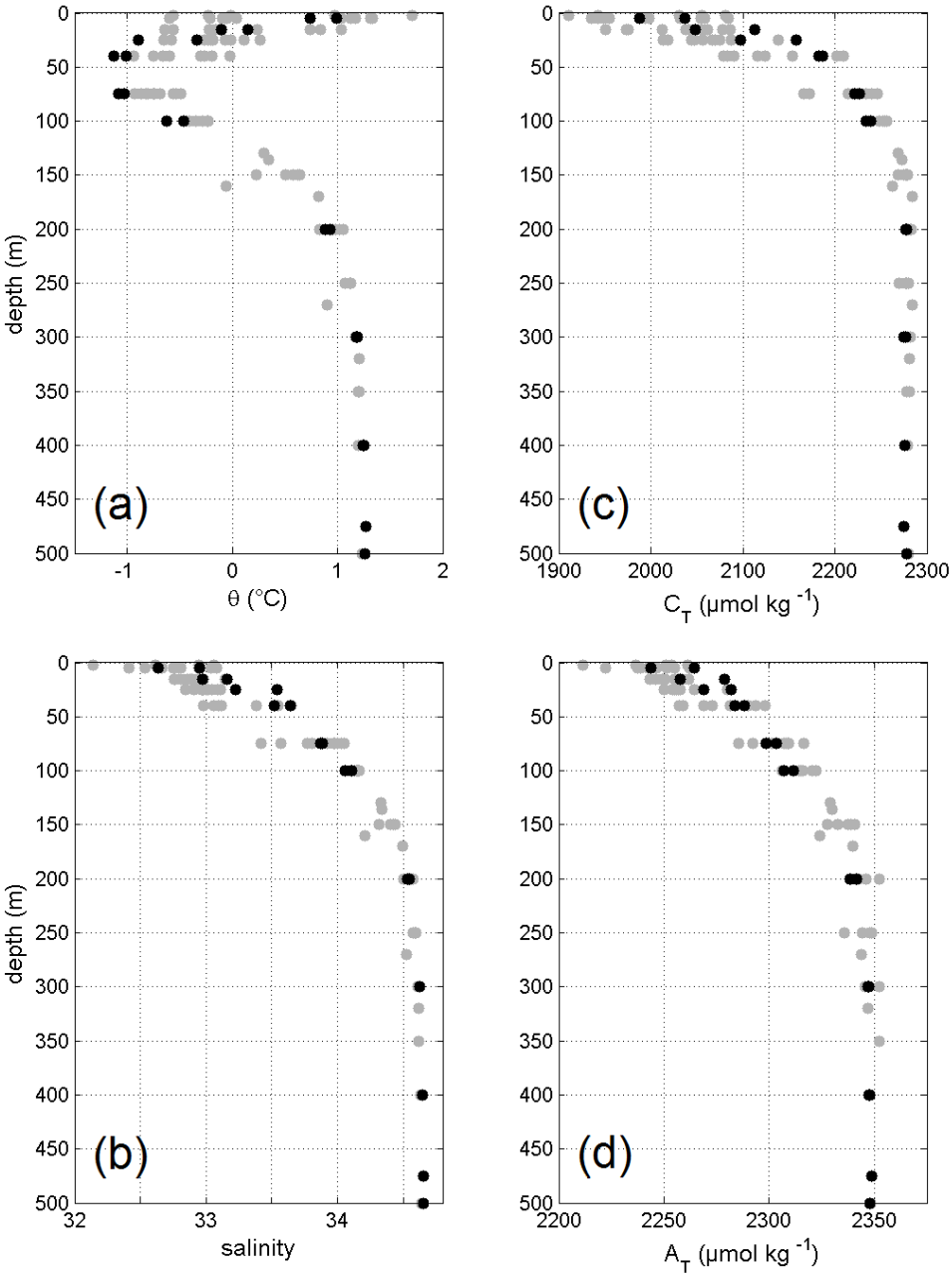
depth (m)
0
50
100
150
200
250
300
350
400
450
500
(a)
-1
0
1
2
θ (°C)
(c)
1900
2000
2100
2200
2300
C_T (μmol kg $^{-1}$)
(b)
32
33
34
salinity
(d)
2200
2250
2300
2350
A_T (μmol kg $^{-1}$)